



Sedimentation, tectonic subsidence and hydrocarbon maturation history of the Gabes-Tripoli Basin, western offshore, Libya

Ibrahim Y. Mriheel

Exploration Department, National Oil Corporation, P. O. Box 2655, Tripoli, Libya

E-mail address: imriheel@noc.ly

Highlights

- This paper provides comprehensive synthesis of the sedimentation and tectonic history of the Gabes-Tripoli Basin, Western offshore of Libya. HC maturation history has also been investigated and explained in the light of the tectonic setting and thermal regime of the basin.
- The paper provide new paleogeographic maps, new thermal regime maps, new HC maturation maps and tectonic model explaining Gabes-Tripoli Basin, Western Libyan Offshore formation and evolution history.
- New paleogeographic maps constructed based on chronostratigraphic well-well correlations can be used for petroleum paly fairway analysis.
- New corrected thermal regime maps can be used for HC maturation analysis of the Gabes-Tripoli Basin.
- The thermal regime of the Gabes-Tripoli Basin, Western Libyan offshore has been constructed considering spatial crustal thickness variation and corrected Bottom-Hole Temperatures.
- Tectonic model proposed explaining Gabes-Tripoli Basin formation and evolution.

ARTICLE INFO

Article history:

Received 01 February 2018

Revised 30 May 2018

Accepted 06 June 2018

Available online 31 March 2019

Keywords:

Sedimentation, Tectonic subsidence, HC maturation history, Libyan offshore

ABSTRACT

The Gabes-Tripoli Basin (G-T Basin) is a Mesozoic-Cenozoic basin which was initiated as a result of widespread, middle Triassic, Jurassic and early Cretaceous extensional movements that developed over a broad zone of strain between the African and European plates.

The sedimentary succession in the G-T Basin ranges in age from Triassic-Recent. The tectono-stratigraphic units comprise of 7 main second-order sequences reaching a 10 km-thick succession of Early-Middle Triassic, non-marine and marine clastics, late Triassic-Middle Jurassic, predominantly shallow marine carbonates and evaporites and Middle Jurassic-Recent marine carbonates and clastics.

The analysis of the basin-fill history of the G-T Basin from the Triassic until the Holocene reveals that the basin underwent development from a continental sedimentary basin located on Gondwana to an epicratonic rift basin. When main Mesozoic extensional movements ceased, the basin subsided thermally and developed as part of a passive continental margin on the North African plate margin. The basin has been subjected to compressional movements lead to inversion during late Cretaceous and Eocene time.

The dominant driving mechanism of subsidence seems clear to have been subsidence due to cooling following lithospheric thinning and the tectonic subsidence history shows that a simple stretching model successfully predicts the overall characteristics of the long-term patterns of the tectonic subsidence of the basin.

The central and northern regions of the basin have similar stretching values; however, the central area is characterized by older timing of HC generation and shallower depth of oil window. In other words, the crustal nature contributing to the heat flow spatial variation and depth of burial influence the changes in the level of HC window within the G-T Basin.

Geochemical analysis and basin modelling have confirmed the source potentiality of the early Eocene-late Cretaceous sequences to generate and expel hydrocarbon in the study area. Hydrocarbon has been generated in a wide span of time from several proven late Cretaceous-early Eocene organic-rich sources. However, none of the sequences younger than the early Eocene had the capability to expel out hydrocarbon in the basin.

1. Introduction

The G-T Basin, in northwestern Libya offshore (Fig. 1), is one of the Mesozoic-Cenozoic sedimentary basins on the North African continental margin. It was formed as a result of extensional tectonic movements that commenced during Triassic and continued during Jurassic and Early Cretaceous. These rifting phases are affecting other Mediterranean regions in the Pelagian and Ionian Seas (Finetti, 1982). Late Cretaceous – Eocene witnesses compressional tectonic phases lead to basin inversions. The ultimate Oligocene-Quaternary rifting phase has resumed its activity and was accompanied by strike-slip movements (Mriheel and Alhnaish, 1995).

Fig. 2 shows the location of the study area and the drilled exploration wells used in correlations, facies analysis and paleogeographic reconstruction of depositional sequences. In this study, the subsurface analysis of the whole succession within the G-T Basin was carried out to unravel the subsurface aspects of the different depositional sequences and to interpret the overall basin evolution history. In this study, the tectonic subsidence history of the basin has been analysed and a tectonic model explaining the observed subsidence history and basin initiation mechanism has been proposed. The thermal maturation history will be analysed and the consequent hydrocarbon windows pattern will be discussed, providing insight into the hydrocarbon prospectively of the basin.

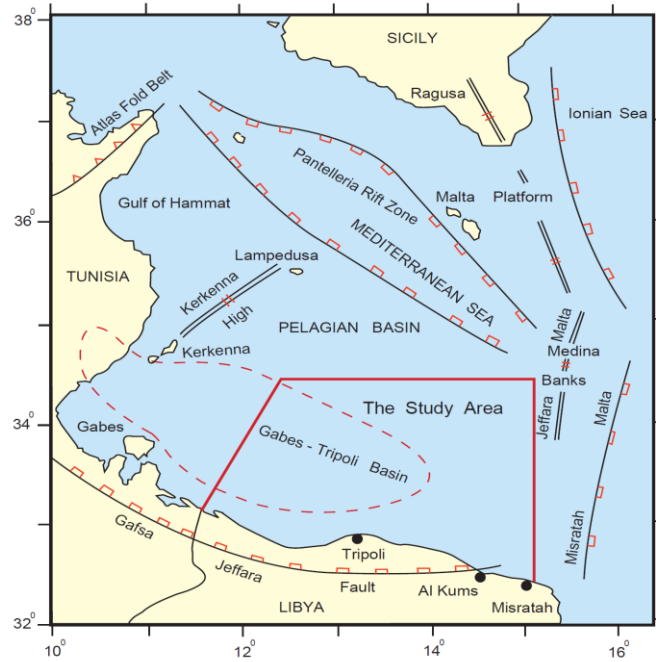


Fig. 1. Map showing the study area relative to the Pelagian Basin

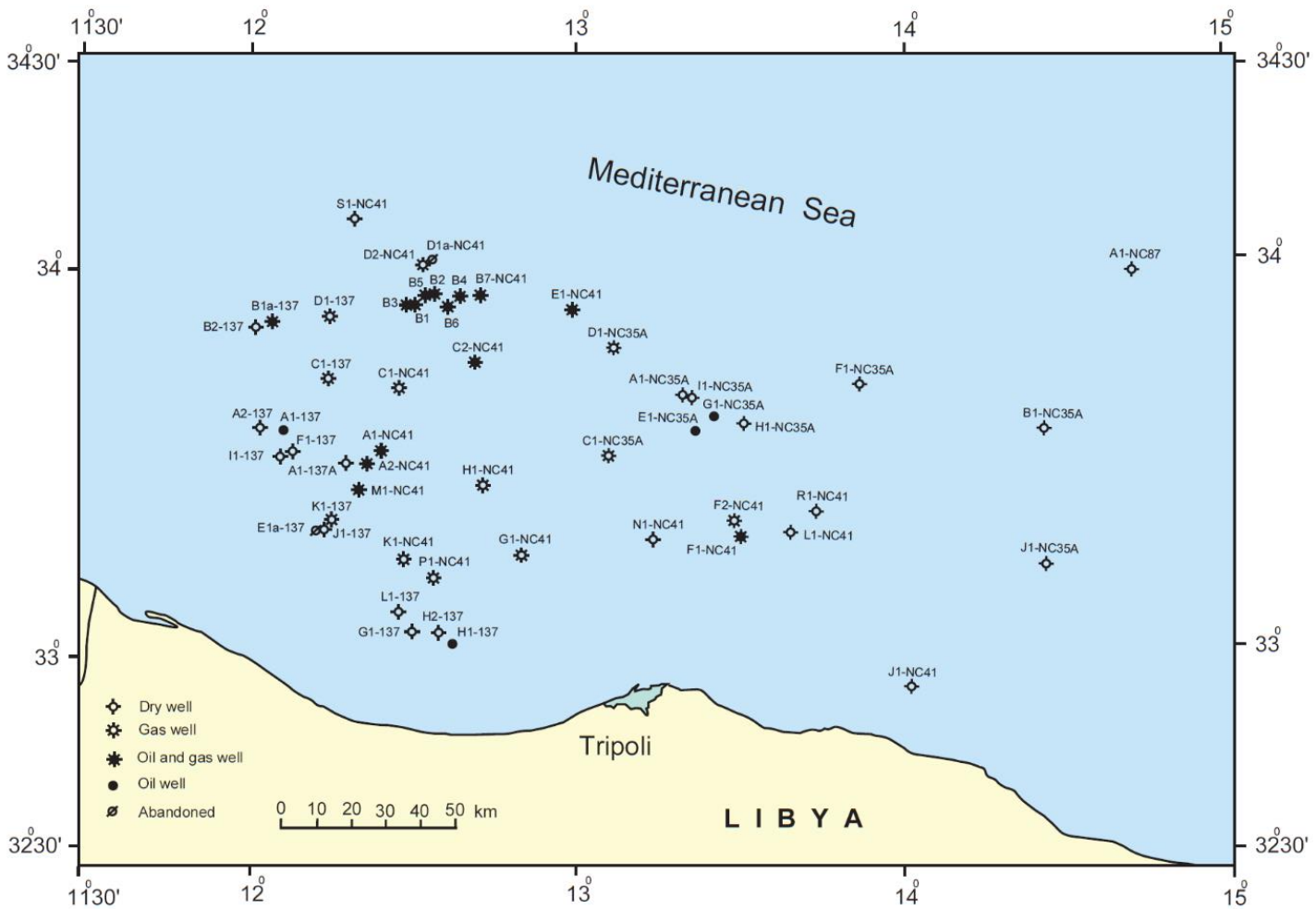


Fig. 2. Location map showing the distribution of the studied wells

1.1 Data and methods

This study presents an integrated basin analysis study involving subsurface geological and geophysical data, basin subsidence, thermal regime and maturation history analyses. The study utilises a multi-disciplinary approach to the problem of identifying and investigating the factors that control basin initiation, thermal regime, maturation history and hydrocarbon accumulations. Thus, the study uses a wide variety of techniques and draws on data obtained from geophysical well logs, seismic, and geological data.

1.1.1 Subsurface analysis

The subsurface study of the whole succession within the G-T Basin was carried out to unravel the subsurface aspects of the different depositional sequences and to interpret the overall basin evolution history. In order to investigate the G-T Basin evolution in the light of the global tectonic regime, a different approach from previous studies was followed to explain the stratigraphy, sedimentation history and mechanism of basin formation. The method simply involves the subdivision of the whole sedimentary succession into tectonostratigraphic mega sequences, all of which are linked in one way or another to regional tectonic episodes that can be correlated with the Mediterranean basin tectonic history. Thus, it was possible to interpret the development of the different depositional sequences and their bounding hiatuses in terms of relationships to eustatic sea level changes and regional tectonics. To fulfil the planned objectives, after well to well correlation had been achieved, and tops throughout the whole succession were calculated, a series of subsurface maps and diagrams were prepared. The constructed maps and diagrams include facies maps; palaeogeographic maps; isopach maps; structural maps and depositional models.

1.1.2 Basin subsidence history analysis

This part of the study involves numerical analysis of the basin subsidence history based on stratigraphic data obtained from drilled boreholes within the basin. The one-dimensional basin modelling software (Genex) of the French Institute of Petrol (IFP) was used to model subsidence in the G-T Basin. Subsidence analysis or backstripping was carried out at various localities within the region using lithologic and stratigraphic information from exploration wells. The tectonic subsidence can be estimated by quantitatively removing the effects of subsidence caused by sediment loading and basin water-depth changes.

Basins subsidence in the G-T Basin was reconstructed using a 'standard' method and the procedure used is similar to that of Steckler and Watts (1978). The 24 sites used for backstripping analysis were carefully selected from 50 available exploration wells. Using subsurface data and seismic lines as a guide, only those wells without significant faulting, or possible disruption by salt movement, were chosen. The location of the selected wells encompasses the overall tectonic evolution across the basin. Stratigraphic thicknesses and lithologic data were obtained from exploration geophysical well logs. Estimates of palaeobathymetry is based on palaeontological assemblages and sedimentary facies. Total subsidence of the stratigraphic column was corrected for sediment compaction. Tectonic subsidence was further corrected for the load effect of the sediments on total subsidence, using a one-dimensional Airy isostatic model, and is intended to reflect the tectonic forces driving basin subsidence. The amount of tectonic subsidence was computed and subsidence curves were automatically constructed.

1.1.3 Hydrocarbon maturation history

Burial history curves were constructed for 44 wells to evaluate the thermal and maturation history of the basin. The burial curves and thermal maturity calculations were made using Genex, developed by Institute Francais du Petrole (1995). This uses the kinetic maturity models developed by Tissot and Espitalie (1975) and Ungerer *et al.*, (1988) and can account for any burial history, geothermal gradient and various types of organic matter represented by a

range of activation energies. The burial history curves are representative of the different thermal scenarios across the G-T Basin. The results should be considered as reliable, given the fact that all exploration wells from this large basin were examined in detail. Thermal histories of the drilled wells from the G-T Basin were first evaluated using the corrected measured temperatures to generate a range of thermal histories compatible with the observed TAI and Tmax data. Calibrating heat flow and thermal conductivity to match observed subsurface temperatures is frequently done in thermal modelling. When there are no other thermal indicator data (e.g. vitrinite reflectance, T_{max} , TAI) to calibrate the model, the fit to present-day temperatures is the only measure of the accuracy of the thermal model (McKenna and Sharp, 1998). Maturation reliability is confirmed by the predicted vitrinite values since these are in accord with the observed data. Finally, this work has seen a determination of all factors that controlled the petroleum generation and migration within the G-T Basin with mapping of the oil windows, and determination of the time of petroleum generation. The migration pathways have been constructed from palaeoheat flow anomalies, structural and seismic time maps on the top of the principal reservoir rocks.

2. Geological setting

The G-T Basin is located on the passive continental margin offshore the city of Gabes and Tripoli and oriented in an east-west direction, parallel to the NW Libyan coastal line (Fig. 1). The basin is about 400 km long and 170 km wide and covers an area of approximately 60 000 km². To the north, the basin is bounded by Malta – Medina Plateau and, to the south; it is bounded by the Jefarah Plain.

The tectonic evolution of the G-T Basin is dominated by Mesozoic rifting of the northern African margin, resulting in the break-up of Pangaea and resulting in the development of several Mediterranean basins (Finetti, 1982). Deposition of the Mesozoic mega-sequences took place during several rifting phases affecting the Mediterranean basins along the North African plate, starting from Triassic and passing through the Jurassic and terminated during early Cretaceous. The basin witnessed compressional phases during late Cretaceous and Eocene followed by Oligocene-Quaternary rifting (Fig. 3). The tectonostratigraphic evolution of G-T Basin can be subdivided into three cycles (Fig. 3).

- *The pre-rift megasequence:*

The first stage of basin evolution involved uplifting and faulting during the Palaeozoic, which caused erosion of the pre-Triassic sediments and development of a broad arch during the Hercynian orogeny. This phase preceded the break-up of Gondwana, which began in the early Jurassic. During the early Triassic, the pre-rift phase sequence was formed in initially faulted basement blocks and contains continental siliciclastics (Figs. 3 and 4).

- *The rifting megasequences: can be subdivided into three super-sequences.*

The first one is made up of middle-upper Triassic shallow marine sediments, representing the first seawater inflows from the north. This section developed during sea level rise, combined with mild tectonism during Middle Triassic, led to widespread deposition of shallow shelf siliciclastics and carbonates of Kurush and Al Aziziyah Fms respectively (Fig. 3).

The overlying Upper Triassic-Middle Jurassic sequence consists of continental siliciclastics, shallow restricted shelf carbonates to hypersaline lagoonal evaporites and mixed siliciclastics and shallow marine carbonates. This section corresponds to a period of a relatively active tectonics and continuing subsidence indicated by the deposition of a thick admixture of lithologies and development of major erosional boundary during the whole Upper Jurassic (Fig. 3).

The remaining Lower Cretaceous section is characterized by deposition of marginal marine siliciclastic and carbonate, shallow carbonate shelf and deep shelf to basinal settings. On the neighboring onshore vicinity, fluvial sediments are ubiquitous. The start of Lower Cretaceous time witnessed uplifting of the Jifarah Plain

which acted as a source of the clastic influx toward the G-T Basin (Figs. 3 and 4).

- The post-rifting megasequences: is comprised of four main second-order sequences.

The advent of Late Cretaceous marks initially the start of a long period of sea level rise in the basin resulting in the development of a broad Cenomanian carbonate ramp overlain by deep shelf to basinal facies corresponding to the Makbaz, Jamil, Bu Isa and Lower Aljurf Fms. A combination of sea-level rise during the late Cretaceous, corresponding to Haq et al. (1987) eustatic sea-level curve, and tectonism lead to deposition of pelagic shale, marl and carbonates in the deep shelf-basinal environmental setting. This section was locally affected by the Santonian inversion phase, which marks the start of the Mediterranean compressional tectonic event (Fig. 3).

The second one is made up of Paleocene-Lower Eocene shallow shelf carbonates developed over the southern and central parts of the basin and passed northward into its equivalent pelagic facies. During the Palaeocene, the offshore area was subjected to severe regressive episodes concomitant with tectonic uplifting induced by volcanism along the southern margin of the G-T basin. The latest

Palaeocene-early Eocene time witnessed a relatively quiescent tectonic phase, during which the carbonates of the Farwah Group were developed. To the north of the offshore region, the Farwah Group passes into pelagic facies of the Hallab Formation (Fig. 3). The overlying Middle-late Eocene section consists of shallow shelf carbonates and shales of the Tellil Group and its deeper water equivalent Ghalil Formation. The Cenozoic closure of the Neotethys has contributed to the Eocene inversion of the basin (Fig. 3).

The remaining Neogene section represents a shallowing upward sequence that commenced with rapid sea level rise and flooding during Oligocene-early Miocene. This leads to deposition of the pelagic facies and development of Dirbal reefal carbonates over local highs. The subsequent increase in clastic influx augmented by subsidence leads to deposition of a muddy shallow shelf with sandy beach sediments of the Al Mayah Formation (Fig. 3). The Tortonian time witnessed quiescent tectonics that encouraged the resumption of carbonate deposition. The end of the sequence is marked by a lowering of the sea level concomitant with the Messinian crises that lead to the deposition of the sabkha-restricted shallow shelf evaporites and carbonates. The sedimentary sequence of the G-T Basin ends with shallow siliciclastic shelf of Pliocene-Recent age (Fig. 3).

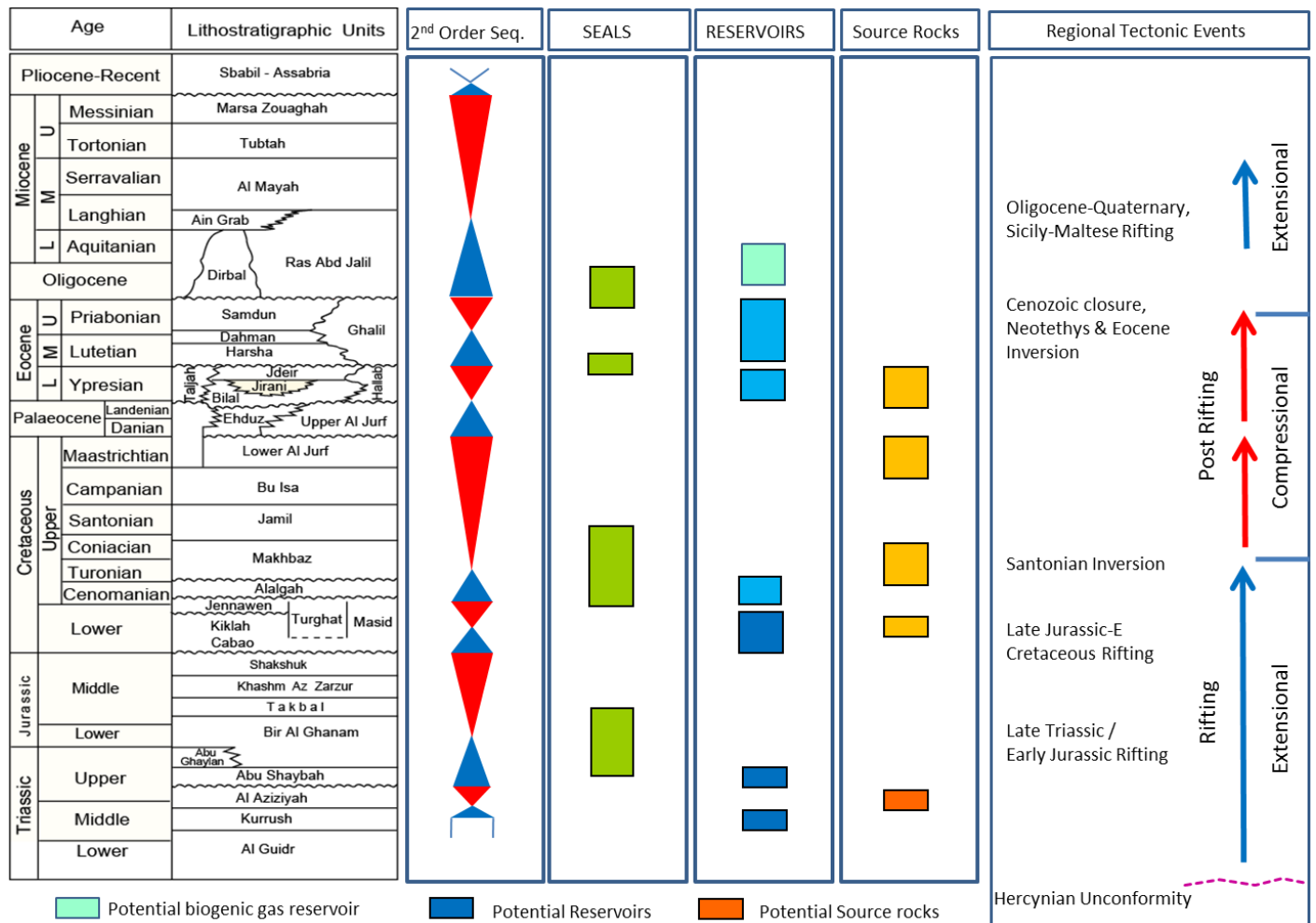


Fig. 3. Showing the G-T Basin Stratigraphy, regional tectonic events and petroleum plays, after Mriheel, 2014 and 2017.

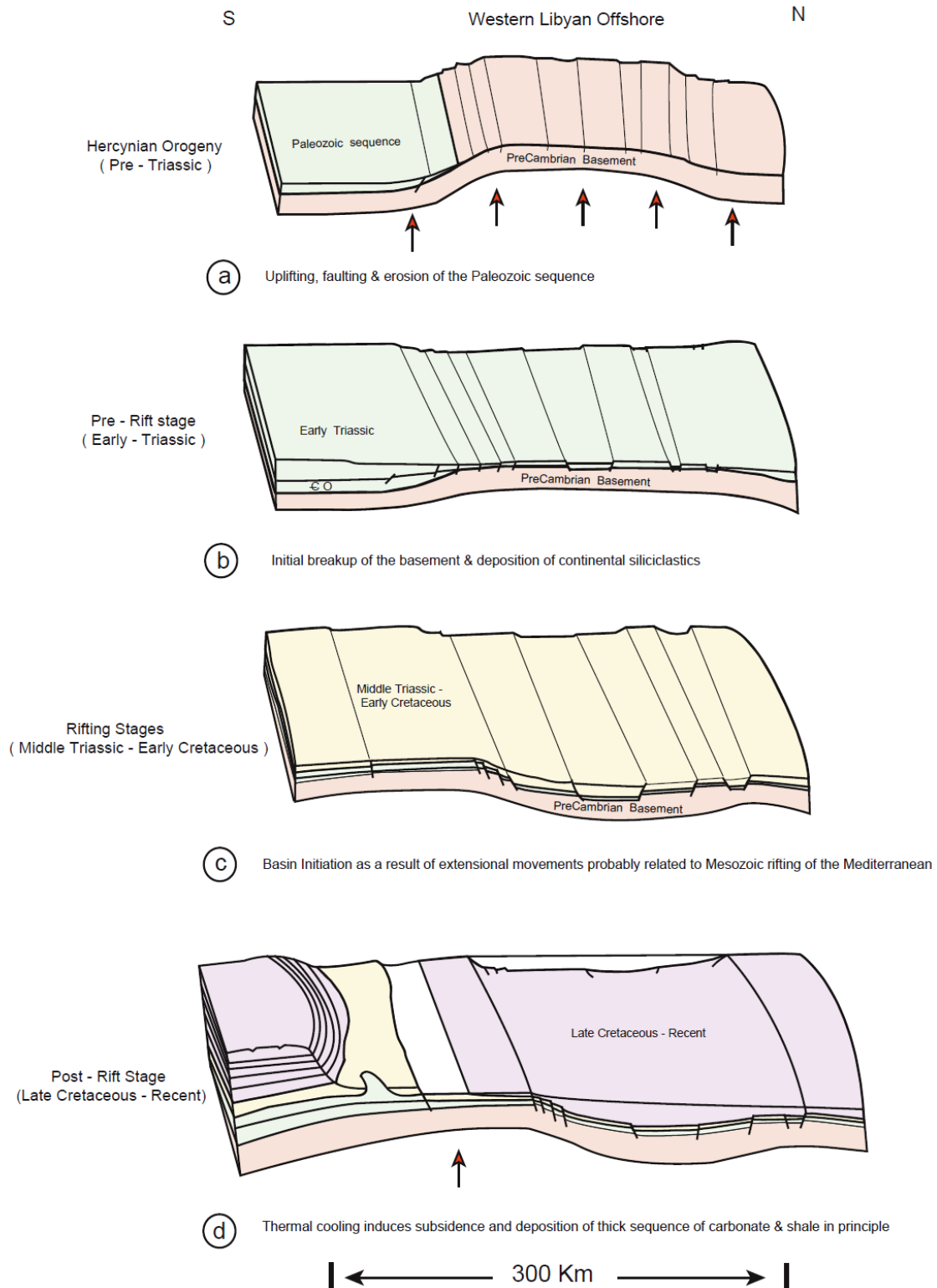


Fig. 4. Summary of the Evolution of the Gabes-Tripoli Basin

3. Stratigraphy and sedimentation history

The sedimentary succession in the G-T Basin ranges in age from Triassic- Recent. In this study, the basin stratigraphy and evolution have been discussed based on global tectonic events linked with the break-up of the Gondwana land, opening of the Atlantic Ocean, and motion of the African plate. The sedimentation history and basin evolution are explained in pre-rift, rifting, and post-rifting stages (Fig. 3).

The sedimentary sequences forming the bulk stratigraphy of the G-T Basin comprises a 10 km-thick succession of Early-Middle Triassic, nonmarine and marine clastics, Late Triassic-Middle Jurassic, predominantly shallow marine carbonates and evaporites and Middle Jurassic-Recent marine carbonates and clastics. The tectono-stratigraphic units comprise 7 main sequences on the time scale of second-order sequences (Fig. 3). For most sequences and sequence boundaries, either a eustatic or tectonically enhanced origin can be established.

3.1 The pre-rifting megasequence

The first stage of basin evolution involved uplifting and faulting during the Palaeozoic, which caused erosion of the pre-Triassic sediments and development of a broad arch during the Hercynian orogeny (Fig. 4). This phase preceded the break-up of Gondwana and the opening of the Neo-Tethys Ocean, which began in the Early Jurassic (Guiraud, 1998). Based on geophysical data, no sediments of Pre-Triassic age appear to be present in the G-T Basin. The oldest encountered sedimentary succession so far is of Late Triassic–Early Jurassic age (Mriheel, 2000). Therefore, the source of information about the Pre-rift megasequence comes largely from the adjacent outcrops in the Jefarah region to the south and from many boreholes drilled in proximity to the offshore region (Hammuda *et al.*, 1985). The pre-rift sediments in the basin consist of Early–Middle Triassic sandstones and shales of the Al Guidr Formation (Fig. 5). Deposition during this phase was predominantly continental siliciclastics (Hammuda *et al.*, 1985). The Al Guidr sediments overlie the basement and are probably witness to the first sedimentation period to take place in the initially faulted and fractured basin.

3.2 The rifting megasequences

- Middle Triassic-Early Jurassic

The subsequent rise in sea level followed Al Guidr deposition, combined with mild tectonism during Middle Triassic, led to widespread deposition of shallow shelf siliciclastics corresponding to the Kurrush Formation (Fig. 5). In the subsurface, the Kurrush Formation consists of shallow shelf sandstones, and shales, dolomite and limestone (Menning *et al.* 1963). The Kurrush Formation is conformably overlain by the Al Aziziyah Formation and overlies the Al Guidr sandstone with gradational contact (Fig. 3).

During the subsequent phases of Middle Triassic–Early Jurassic rifting, the major faults and structural elements of the G-T Basin were either initiated or rejuvenated and significant subsidence of the basin allowed major sedimentation of shallow shelf carbonates and fluvial-shallow marine siliciclastics and restricted shelf-hypersaline lagoon evaporites of the Al Aziziah, Abu Shybah and Bir Al Ganam formations respectively (Fig. 5).

This late Triassic–Middle Jurassic tectonic activity laid the foundation of the extensional G-T Basin on the northern margin of the African Craton. This phase was concomitant with the break-up of Gondwanaland and the opening of the Atlantic Ocean (Guiraud, 1998).

- Middle Jurassic

At the western Libyan offshore area, Middle Jurassic is represented by the upper Bir Al Ghanam, Takbal, Khashm Az Zarzur and Shakshuk formations (Fig. 3) and is comprised of shallow restricted shelf sandstone, siltstone and shale, evaporates, dolomites and limestones. The subdivision of these lithostratigraphic units is well established in the neighboring area of Jifarah Escarpment. However, due to scarce subsurface information about deeper sequences, hence their subdivision remained arbitrary.

- Early Cretaceous

The last event of Mesozoic rifting is corresponding to the Lower Cretaceous phase (Figs. 3 and 4). The advent of Early Cretaceous time witnessed uplifting of the Jifarah plain, which acted as a source of the clastic influx toward the G-T Basin (Mriheel, 2000). Early Cretaceous sedimentation continued over the Jifarah Plain with fluvial deposits of the Kiklah Formation (Fig. 5). On the offshore shallow

shelf environments are ubiquitous. At the end of the Early Cretaceous (Aptian–Albian), Kiklah, Turghat and Masid formations were deposited (Figs 3 and 5) and are comprised of marginal marine siliciclastic and carbonate, shallow carbonate shelf and deep shelf to basinal settings respectively (Fig. 5). This stage was contemporaneously occurred with Sirt basin rifting. Differential block movements toward the offshore that followed the Kiklah deposition continued as the area was invaded by the Late Cretaceous sea. Initial transgression was first started during Late Albian–Early Cenomanian as the marginal marine sediments of the Jennawen Formation would suggest (Mriheel, 2013 and 2014).

3.3 The post-rifting megasequences

- Late Cretaceous

The advent of Late Cretaceous marks initially the start of a long period of sea level rise in the basin resulting in development of abroad Cenomanian carbonate ramp corresponding to the Alalghah formation (Fig. 5). Progressive transgression continued from Turonian to Maastrichtian and lead to the deposition of the deep shelf to basinal facies corresponding to the Makbaz, Jamil, Bu Isa and Lower Aljurf formations (Figs 3 and 5). A combination of sea level rise during the Late Cretaceous, corresponding to the Haq *et al.* (1987) eustatic sea level curve, and tectonism lead to deposition of pelagic shale, marl and carbonates in deep shelf-basinal environmental setting. This section was locally affected by the Santonian inversion phase (Fig. 3) which mark the start of the Mediterranean compressional tectonic event.

During the Late Coniacian, the western Libyan Coastal Fault system and structural elements of the basin were rejuvenated. As a result, the Jifarah Plain emerged as a landmass, and significant sedimentation onshore is thought to have ceased since then. This continuous rise in sea level and rejuvenation of the western Libyan coastal fault system appears to have slightly exceeded the uplift of the peripheral palaeohigh around the G-T basin. Consequently, a long period of non-deposition and erosion persisted over the emergent area of the Jifarah Plain (Mriheel, 2000).

- Tertiary

Subsequent to the deposition of the Maastrichtian shales, the depositional style in the G-T Basin changed as a prism of shallow-marine sediments prograded seaward across the basin. This broad progradational wedge defines the shallowing Tertiary depositional sequences, which range in age from the Palaeocene to Recent (Fig. 3). The shallowing Tertiary deposits encompass three main second order depositional sequences: Late Palaeocene–Early Eocene, Middle–Late Eocene, and Oligocene–Late Miocene (Fig. 3). The later is capped by thin and incomplete sequence of Pliocene–Recent age (Fig. 3). These depositional sequences are characterised by several stacking patterns during their development and throughout the Tertiary period, shallow shelf carbonates and siliciclastics predominate the southern region. To the north, in deeper water, shales, marls and limestones were deposited in deep shelf–basinal setting (Figs. 6 and 7).

During the Palaeocene, the offshore area was subjected to severe regressive episodes concomitant with tectonic uplifting induced by volcanism along the southern margin of the G-T basin. This was accompanied by exposure of the Late Cretaceous sequence toward the southern margin of the basin and deposition of a narrow belt of Ehduz shallow shelf carbonates and its equivalent pelagic facies of Upper Al Jurf Formation (Fig. 6).

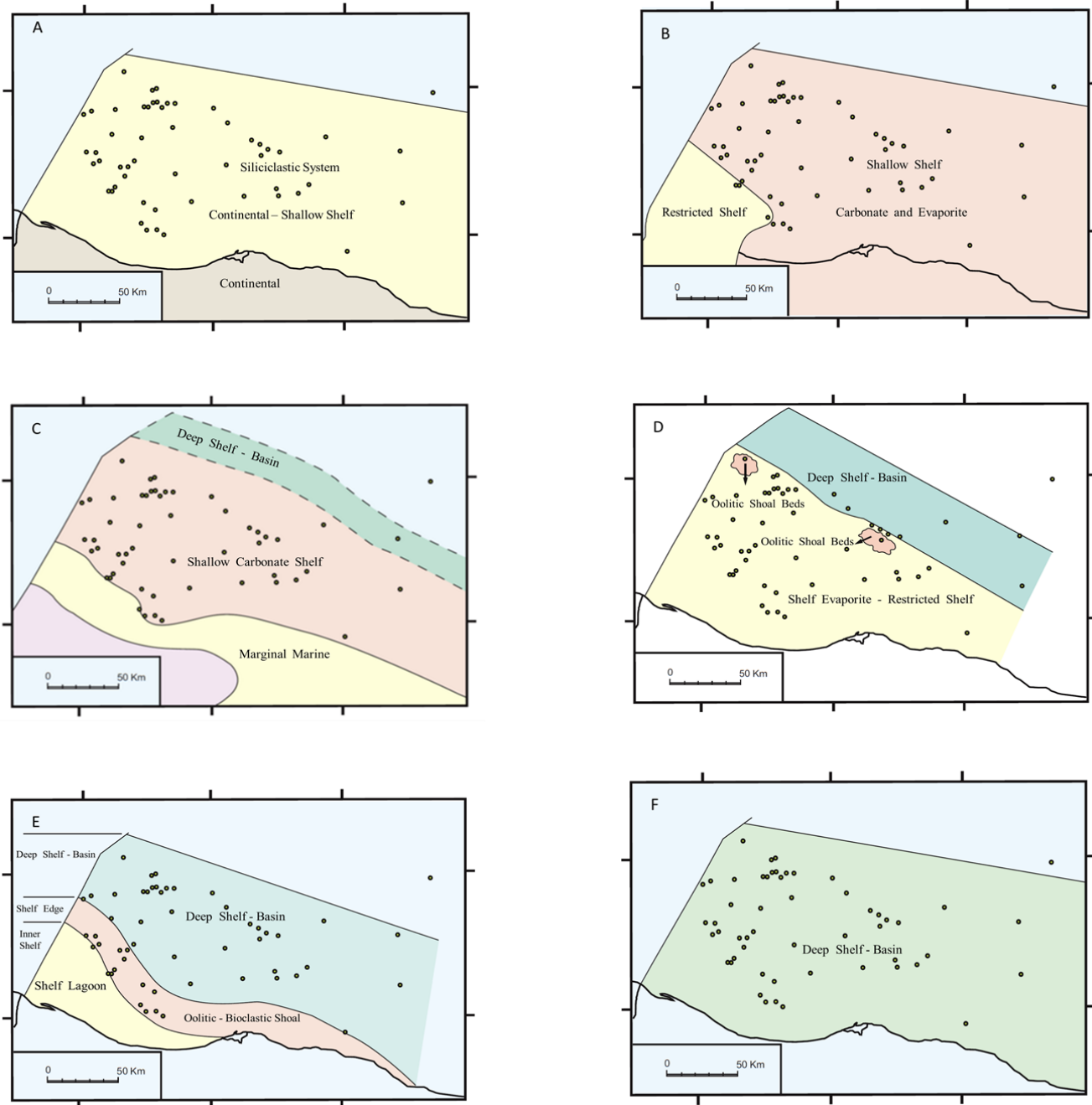


Fig. 5. Showing the paleogeography of the Mesozoic Megasequences. (A) Main facies and depositional environment of the early-middle Triassic AlGuidr-Kurrush Fms. (B) Depositional environment of the Al Aziziyah, Abu Shaybah and Bir Al Ghanam Fms during late Triassic-middle Jurassic. (C) Main depositional settings and facies belts of the early Cretaceous Kiklah, Turghat and Masid Fms. (D) Depositional facies and environment of the Cenomanian Alalghah Fm. (E) Main facies belts and environments of the Turonian- Coniacian Makbaz Fm. (F) Depositional environment of the Santonian-Maastrichtian Jamil, Bu Isa and Lower Al Jurf Fms.

The latest Paleocene-Early Eocene time witnessed a relatively quiescent tectonic phase, during which the carbonates of the Farwah Group were developed over the southern and central parts of the basin. To the north of the offshore region, the Farwah Group passes laterally into its equivalent pelagic facies of the Hallab Formation (Fig. 6). After a short period of erosion or non-deposition of the early Eocene sediments, sedimentation resumed with the rise of sea level in the Middle Eocene. The Middle-Late Eocene shallow shelf intercalations of carbonates and shales of the Tellil Group and its deeper water equivalent Ghalil Formation were developed (Fig. 6). Again, after uplifting and erosional event related to the closure of the Neotethys during Eocene inversion (see Fig. 3), a shallowing upward sequence that commenced with rapid sea level rise and flooding during Oligocene-Early Miocene was established. The Oli-

gocene-Miocene sequence is bounded by obvious hiatuses and consists of the RasAbdJalil, Dirbal, Al Mayah, Tubtah, and Marsa Zouaghah formations (Fig. 7; Mriheel, 2000 and 2014).

The subsequent increase in clastic influx augmented by subsidence lead to deposition of a muddy shallow shelf with sandy beach sediments of the Al Mayah Formation (Fig. 7). The Tortonian time witnessed quiescent tectonics that encouraged the resumption of carbonate deposition of the Tubtah Formation (Fig. 7). The end of the Miocene section is marked by a lowering of the sea level concomitant with the Messinian crises that lead to the deposition of the sabkha-restricted shallow shelf evaporites and carbonates of the Marsa Zouaghah Formation (Fig. 7). The sedimentary sequence of the G-T Basin ends with siliciclastics of Pliocene-Recent age. The sequence is represented by the Sbabil and Assabria formations (Fig. 7).

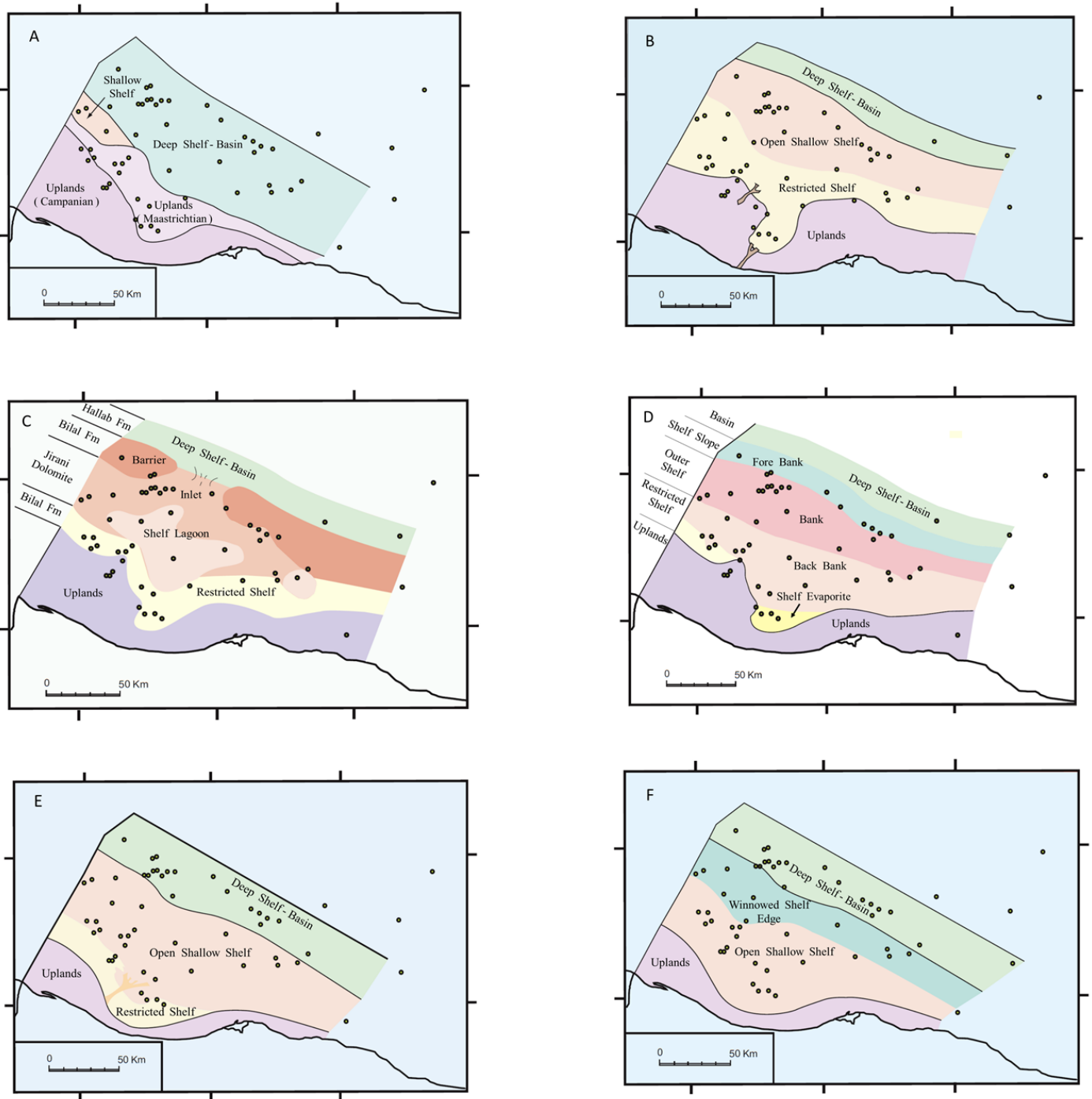


Fig. 6. Showing the paleogeography of the Early Tertiary Megasequences (Paleocene-Middle Eocene). (A) Main facies and depositional environment of the Paleocene Halab Fm. (B) Environmental settings and facies belts of the late Paleocene-early Eocene Bilal Fm. (C) Main depositional settings and facies belts of the Jirani Dolomite and its equivalent upper Bilal Fm. (D) Facies belts and depositional environment of the early Eocene Jdeir, Taljah and Hallab Fms. (E) Main facies belts and environments of the middle Eocene Harash Fm. (F) Main facies belts and depositional environment of the middle Eocene Dahman Fm.

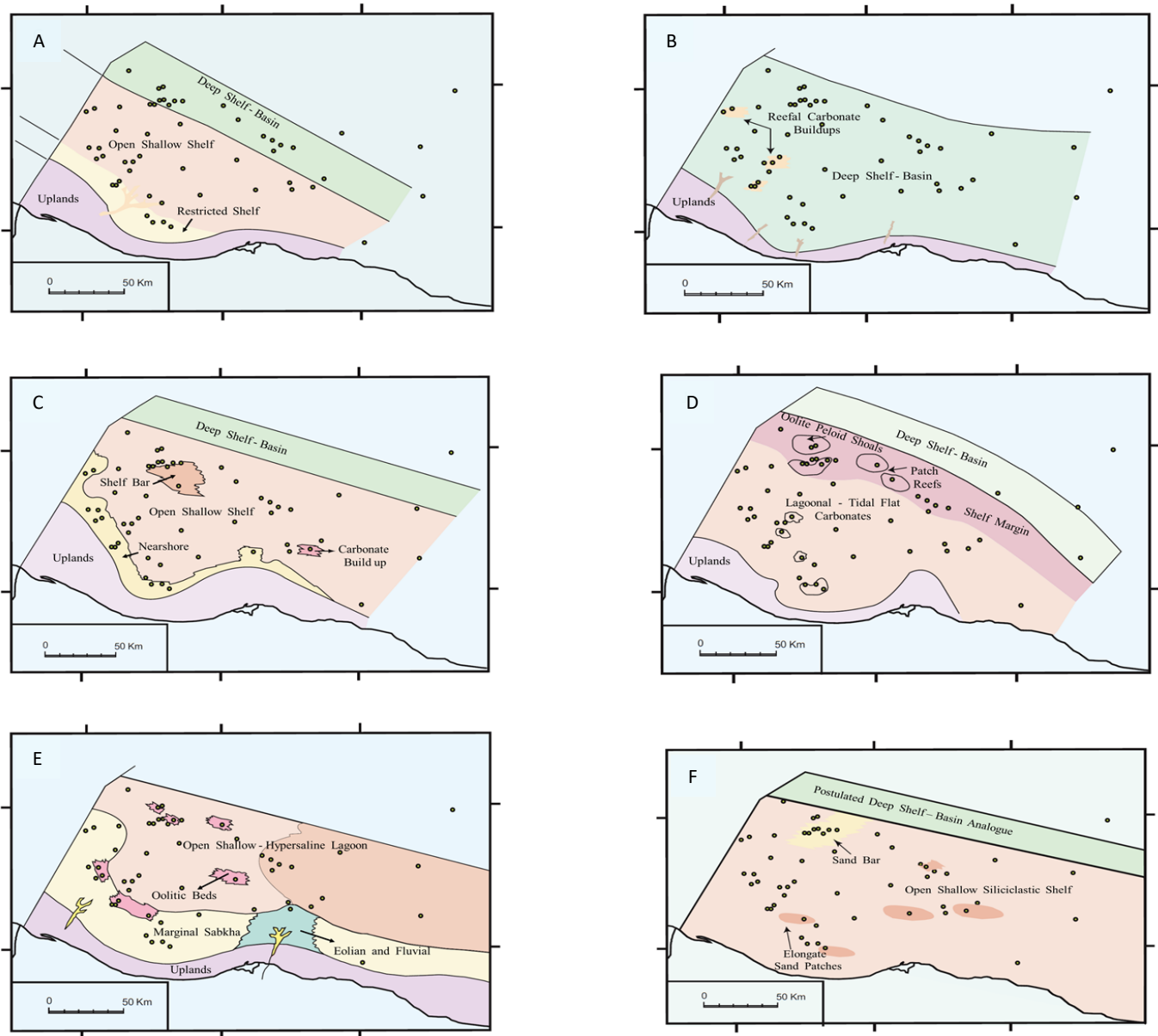


Fig. 7. Showing the paleogeography of the Late Tertiary Megasequences (late Eocene-Recent). (A) Main facies belts and depositional environment of the late Eocene Samdun Fm. (B) Depositional environment of the Oligocene-middle Miocene Ras Abd Jalil Fm and its equivalent Dirbal Fm (C) Main depositional settings and facies belts of the middle Miocene Al Mayah Fm. (D) Facies belts and depositional environment of the Tortonian Tubtah Fm. (E) Main facies and depositional environments of the Messenian Marsa Zouaghah Fm. (F) Depositional environment of the Pliocene-Recent Sbabil and Assabria Fms.

4. G-T Basin subsidence history

Tectonic subsidence analyses of selected sites were carried out to compare patterns of subsidence at different areas in the G-T Basin, using standard backstripping techniques similar to that of [Steckler and Watts \(1978\)](#) and was carried out at 24 localities within the G-T Basin using lithologic and stratigraphic information from exploration wells. The 24 sites used were carefully selected from 50 available exploration wells ([Fig. 8](#)). Stratigraphic thicknesses and lithologic data were obtained from exploration geophysical well logs. Estimates of palaeobathymetry are based on palaeontological assemblages and sedimentary facies. Total subsidence of the stratigraphic column was corrected for sediment compaction. Tectonic subsidence was further corrected for the load effect of the

sediments on total subsidence, using a one-dimensional Airy isostatic model, and is intended to reflect the tectonic forces driving basin subsidence.

Up to the present time, the oldest penetrated succession in the G-T Basin is the Late Triassic-Early Jurassic sediments in well L1-137. Both stratigraphic and seismic data, as well as the constructed subsidence curves ([Figs. 9-11](#)), reveals that the subsidence of the G-T Basin was induced thermally. The thermal phase of subsidence began in the Late Cretaceous. Thus, the beginning of the thermal sag phase marked the end of the primary stretching phase. The post-Jurassic subsidence of the G-T Basin, after backstripping analysis, fits with the overall pattern of the theoretical subsidence curves predicted for a thermal sag phase that would follow whole lithosphere extension. The basement subsidence curves ([Figs. 9-11](#))

show that the tectonic subsidence in the G-T Basin behaves in accordance with the thermal cooling model of Mackenzie (1978). Thus, the basin subsidence of the G-T basin is attributed to lithospheric extension induced subsidence followed by a long period of exponentially decreasing thermal subsidence as the underlying thinned mantle cooled and thickened. Therefore, the Mckenzie (1978) lithospheric extension model can best explain the basin evolution. The amount of tectonic subsidence was computed and subsidence curves were automatically constructed using Genex software.

4.1 Subsidence curves

The stratigraphic accumulation and tectonic subsidence curves for wells in the G-T Basin are shown in Figures 9-11. These Figures (note scale change) show example curves from three locations, wells J1-NC41 and L1-137 in the south, coastal region, wells H1-NC41 and J1-NC35A from the basin centre and wells A1-NC35A and B1-NC35A from a platform in the northern margin of the G-T Basin. These locations are distant from the areas affected by salt domes and have been selected to represent examples of the tectonic evolution of the basin uninfluenced by halokiniesis. The main results are as follows: Magnitudes of total subsidence, tectonic subsidence and stratigraphic accumulation increase from margins to the basin centre (see also Figs. 12 and 13). Generally, the subsidence curves (Figs. 9-11) show that sediment loading accounts for over one-half of the total observed subsidence. The basement subsidence curves (Figs. 9-11) show that the tectonic subsidence in the G-T Basin behaves in accordance with the thermal cooling model of Mckenzie (1978). Hence, the overall pattern of these subsidence curves (Figs. 9-11) suggests that thermal cooling of the continental lithosphere induced considerable basement subsidence during the post-rift stage. The shape of the tectonic curves shows the thermal subsidence was a result of exponential cooling of the basement with time.

Figs. 9 through 11 show that the regional subsidence in the G-T Basin (during post-rift), which followed the extensional event, is broad and well recognized. As a result, the magnitude and the rate of the basement subsidence curves can be directly compared with the predictive model (Mckenzie, 1978) based on simple stretching. The consistent increase of both basement tectonic subsidence curves with the total subsidence curves supports the fact that basin subsidence during later stages of the post-rift phase is augmented by sediment loading.

The tectonic subsidence curves (basement subsidence) shows that low basement subsidence rates correspond to wells on the southern and northern shoulders of the basin (Figs. 9 and 11). This is also supported by stratigraphic accumulation. Hence, stratigraphic accumulation and total subsidence continued in the central main trough of the basin. Vertical motion continued along major faults bordering the G-T Basin in response to loading in the central rift basin. Examination of the constructed tectonic subsidence curves, which were corrected for compaction and sediment and water loads across the G-T Basin reveals the following results. The total basement subsidence curve at the southern margin, in well J1-NC41 (Fig. 9) shows the subsidence is low (does not exceed 1000 m). This subsidence figure represents the last 84 my. On the contrary, during the last 60 my only a high total basement subsidence of 1600m was observed at the basin depocentre in well H1-NC41 (Fig. 10). At the northern margin of the basin in well B1-NC35A (Fig. 11), 1600 m of total basement subsidence was accounted for by the last 98 my. By considering the time duration difference of the total tectonic basement subsidence across the basin a subsidence rate of 12 m/my, 26 m/my and 16 m/my were calculated for the southern, central and northern parts of the basin respectively. Thus, the rate of basement subsidence from the basin margin to the centre increases in magnitude and indicates differential tectonic subsidence across the basin. The variation of tectonic subsidence is best explained by the variation in the amount of crustal extension in the basin. It was found that the crust thinned by more than half of its

original thickness at the basin centre (H1-NC41) and about a quarter of its original thickness in the south, at the coastal region. In summary, the total unloaded basement subsidence of the G-T Basin reveals that low basement subsidence rate corresponds to wells L1-137 and J1-NC41 (Fig. 9) on the southern margin of the basin and to B1 and A1-NC35A wells (Fig. 11) on the northern margin. However, the maximum total tectonic subsidence rate of the basement corresponds to well H1-NC41 (Fig. 10) on the basin center.

4.2 Estimates of crustal extension

Estimation of the amount of extension across the G-T Basin in this study was achieved from deep seismic reflection (Allen and Allen, 1990, p. 90) and the results are summarized in Figure 13. The constructed subsidence curves (Figs. 9-11) represent the post-rift stage of the G-T Basin and their shape shows the thermal subsidence as a result of exponential cooling of the basement augmented by sediment loading with time. Using deep seismic reflection section (see Figs. 14a and 14b) the amount of crustal stretching across the basin has been calculated and the results achieved suggest an appropriate tectonic model for the basin subsidence mechanism. In order to show the variation in crustal thickness across the basin, both the constructed tectonic subsidence curves and cross section were used as a guide to select the best sites to measure the total sedimentary succession at each chosen location within the basin. Assuming that the pre-stretching original thickness of the crust is 35 km thick in the region and taking into consideration depth changes of Moho across the basin from 32 km below the southern coast and 26 km over other parts of the basin (see Fig. 13) the β factor and crustal thickness variation in the basin has been calculated (see Fig. 13). The following are three selected examples from different parts of the basin. At the southern margin in J1-NC41 location, the G-T Basin contains about 6 km of sediments and Moho is approximately 32 km from the surface. The amount of crustal attenuation, in this case, is estimated to be 1.38, which corresponds to 38% extension of the crust beneath the southern margin.

However, remarkably higher values of crustal extension are found in the central parts of the basin i.e. H1-NC41 location, the thickness of the sedimentary section is 11 km and the Moho rises to 26 km from the surface. The range of the extension factor over the basin depocentre is 2.33, which corresponds to 133% extension of the crust. Toward the northern margin at B1-NC35A location, the total sediment thickness is about 8.3 km and depth to the Moho is 26 km. The range of the extension factor is $\beta = 1.97$, which corresponds to 97% extension of the crust beneath the northern margin. Thus, the proof is established that a stretching-driving mechanism is a valid assumption for the basin formation and that the Mckenzie model accurately accounts for the basin evolution.

4.3 Mechanisms of G-T Basin subsidence

Passive continental margins evolve through the initiation of spreading and divergent plate motion within a pre-existing continent (Falvey and Mutter, 1981). Passive continental margins (Atlantic-type margins) are characterized by seaward thickening prisms of marine sediments overlying a faulted basement with syn-rift sedimentary sequences, often of continental origin. The post-rift seaward-thickening prisms of sediments consist predominantly of shallow water deposits (Allen and Allen, 1990). By comparing the compatibility of the Western Libyan offshore with the subsidence mechanisms and their characteristics, the stretching hypothesis was adopted and the Mckenzie model (1978) is believed to explain the subsidence mechanism of the G-T Basin. Moreover, this is considered as a reliable passive margin tectonic model, which is characteristic of subsidence history and maturation depth. Hence, it can be used as a useful exploration tool on the Western Libyan Continental margin. In the Mckenzie model, a rapid stretching of continental lithosphere produces a thinning and passive upwelling of the hot asthenosphere.

This stage is associated with block faulting and subsidence. The lithosphere then thickens by cooling, and slow subsidence occurs

not associated with faulting. The slow subsidence and the heat flow depend only on the amount of stretching, which can be estimated from these quantities and from the change in thickness of the continental crust caused by the extension. The model is therefore easily tested using the subsidence results, the heat flow interpreted from temperature structure and thermal regime in this study and the form of basement topography as well as variations in Moho relief over the basin (Fig. 13). It is concluded that the Mckenzie (1978) lithospheric extension model is compatible with geological and geophysical data of the G-T Basin and explains its evolution. The following evidence supports the proposed model.

- The overall shape and pattern of the constructed tectonic subsidence curves reveal the exponential decline of subsidence and fit with those developed as a result of thermal cooling of the stretched lithosphere (see Fig. 12).
- The depth changes of Moho across the basin from 32 km below the southern margin of the basin to 26 km over other parts of the basin and thinning of the crust to more than half of its original thickness at the central parts of the basin (Fig. 13) suggests lithospheric stretching is appropriate deriving mechanism of the basin subsidence.

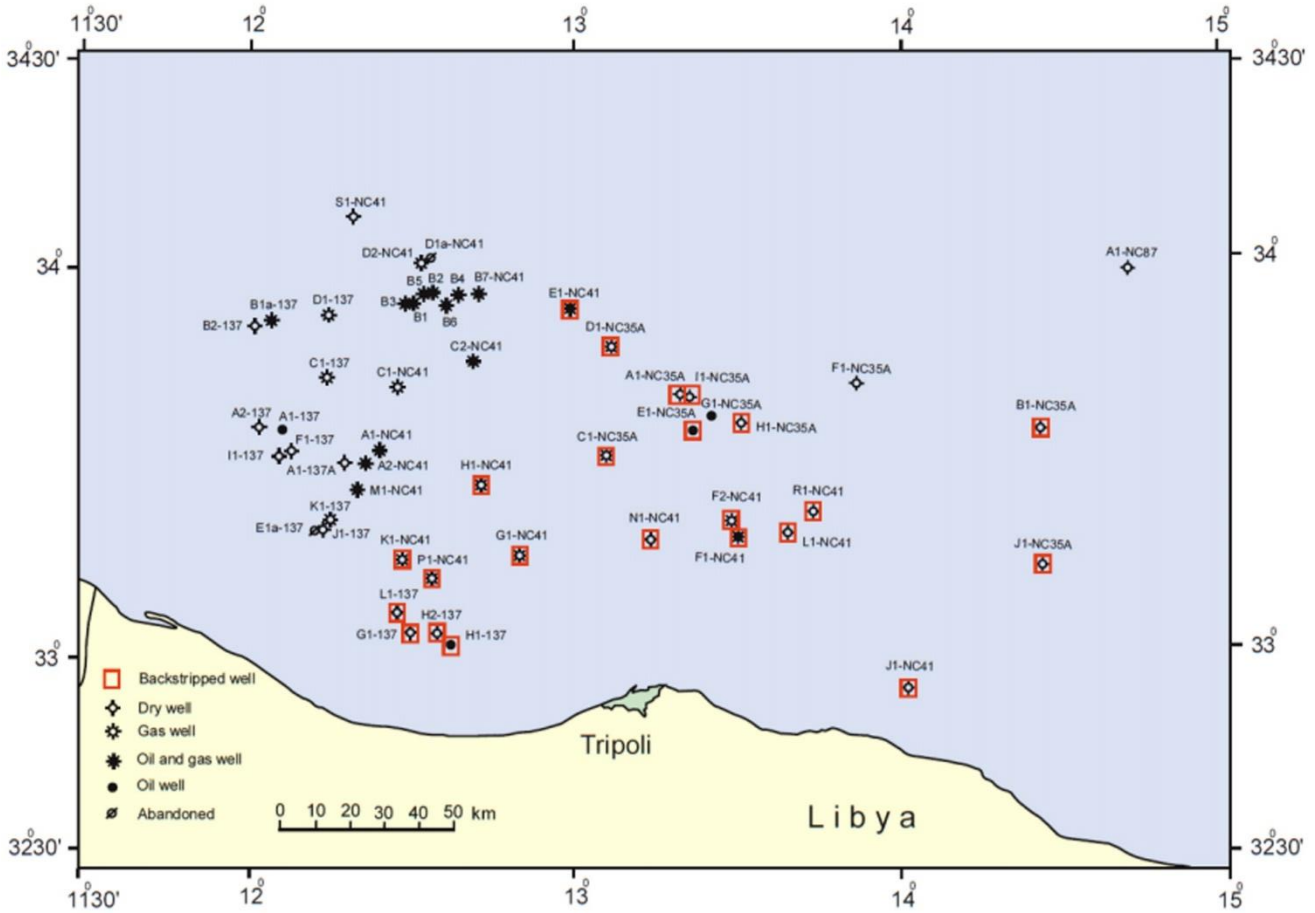


Fig. 8. The selected exploration Wells for backstripping

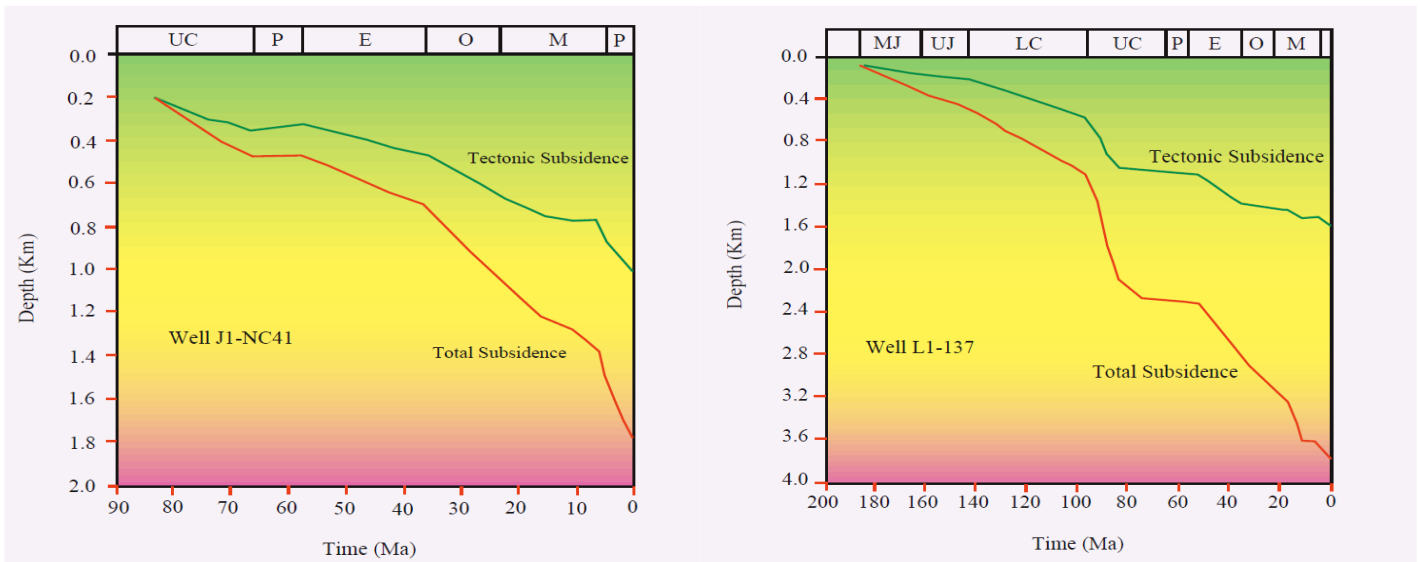


Fig.9. Total and tectonic subsidence curves at the southern margin of the G-T Basin. See Fig. 8 for well location.

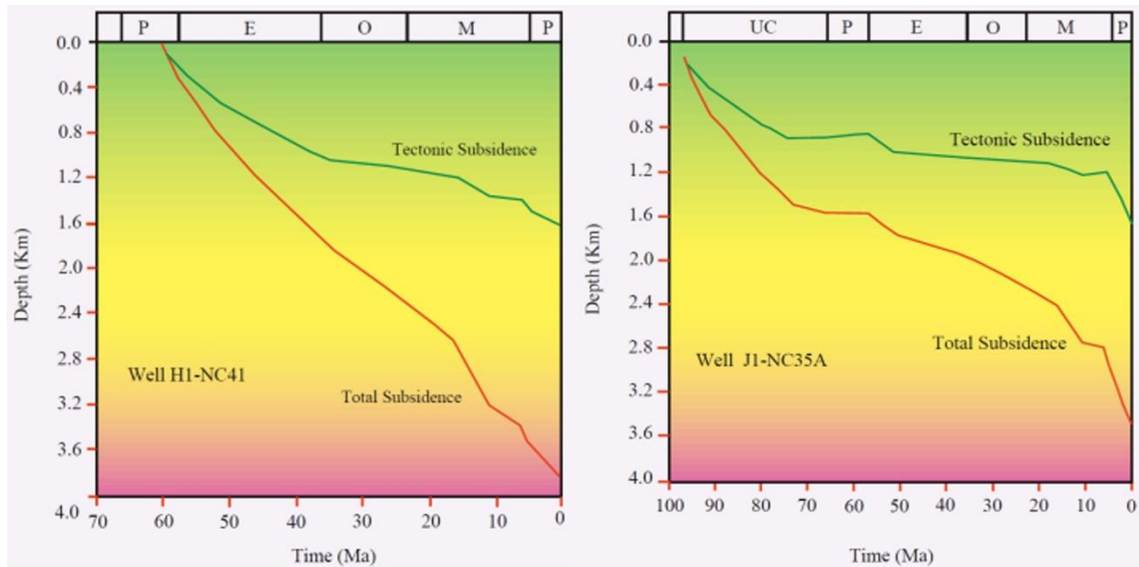


Fig.10. Total and tectonic subsidence curves at the central part of the G-T Basin. See Fig. 8 for well location.

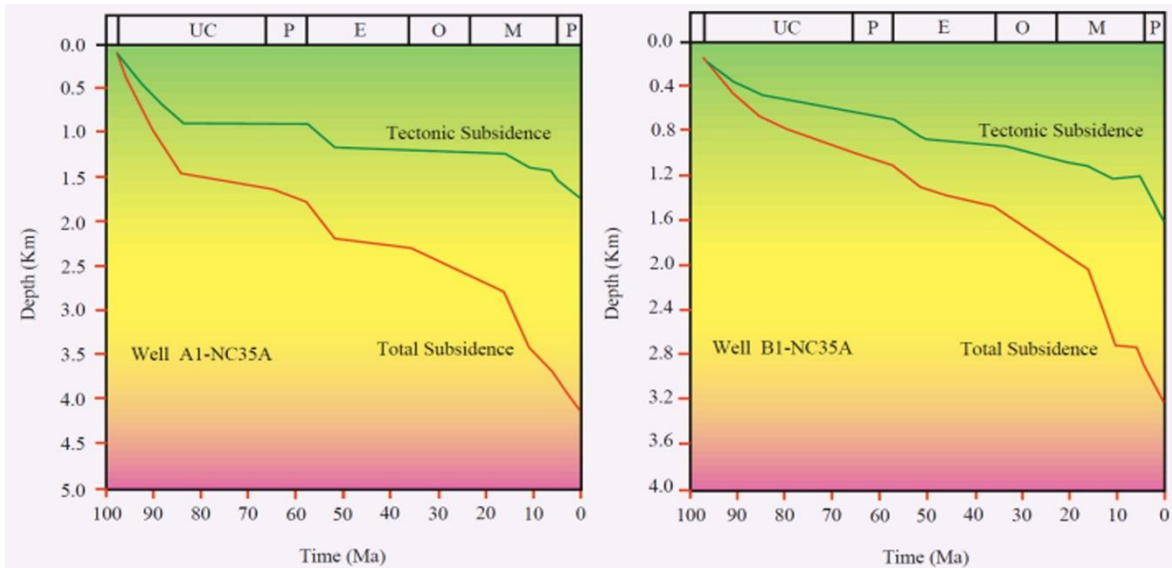


Fig.11. Total and tectonic subsidence curves at the northern margin of the G-T Basin. See Fig. 8 for well location.

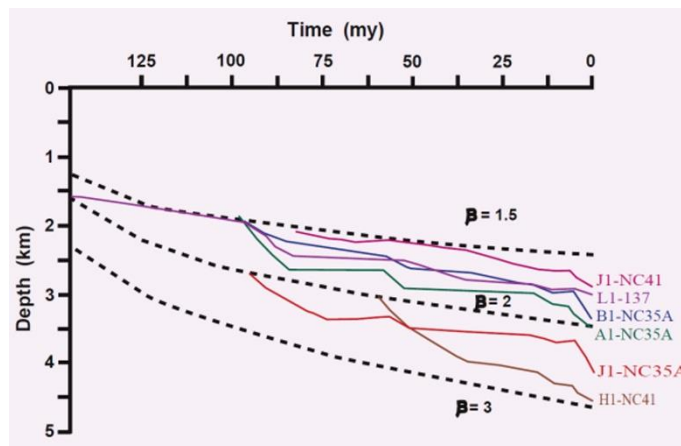


Fig. 12. Comparison between the predictive subsidence model (Beta) and the calculated tectonic subsidence curves at the G-T Basin. See Fig. 8 for well location.

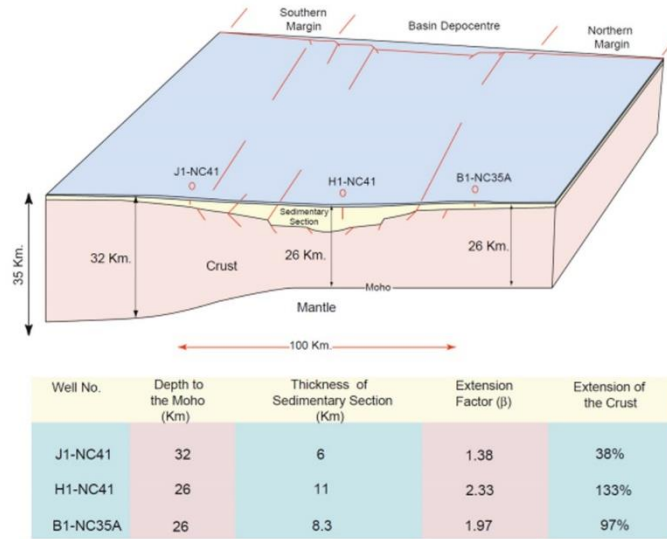


Fig. 13. The β factor of the crustal thickness variation in the basin has been calculated assuming pre-stretching original thickness of the crust is 35 km. thick in the region and considering the depth changes of the Moho across the basin.

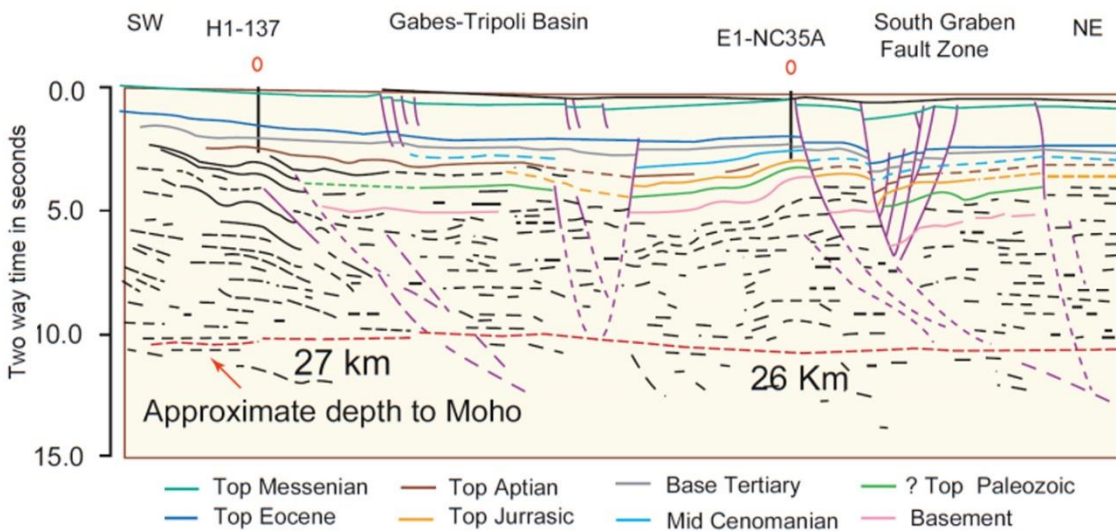


Fig. 14a. Interpreted deep seismic deep reflection section showing the crustal thickness changes across the Gebes-Tripoli basin after (Faux *et al.*, 1988)

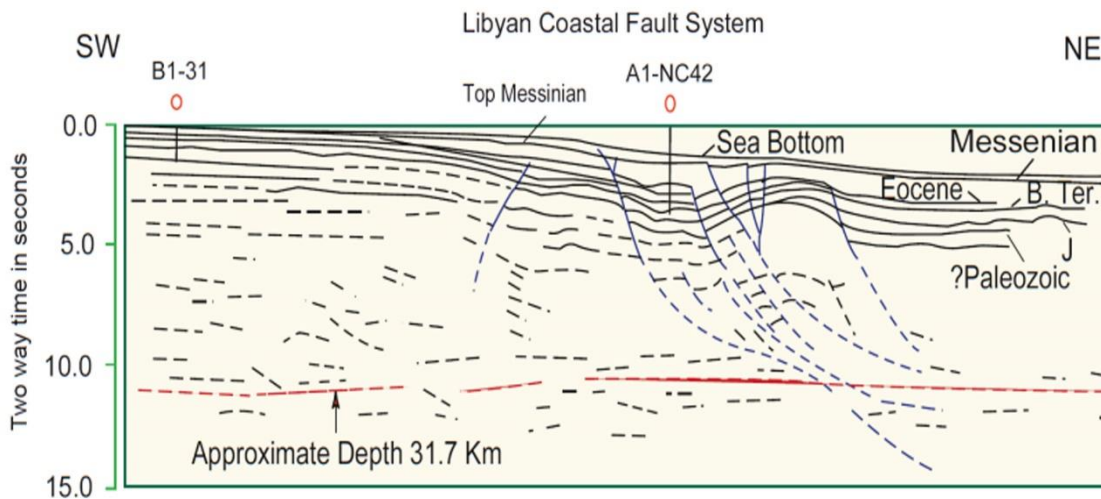


Fig. 14b. Interpreted deep seismic deep reflection section showing the crustal thickness changes across the faulty costal system after (Faux *et al.*, 1988)

5. Hydrocarbon maturation history

Thermal maturation history of the G-T Basin has been conducted in order to reduce exploration risk and enhance future exploration in the offshore area. To fulfill this objective the one-dimensional basin modeling software (Genex) of IFP has been used to model the oil window and time of oil generation in the region. Areas

of potential petroleum source rocks were mapped after correction of the bottom hole temperature (BHT) and the thermal maturation history of the basin was assessed after preparation of new geothermal gradient and heat flow maps (Figs. 15 and 16). Burial history and oil window curves were constructed for all exploration wells and maturation maps of principal source rocks were prepared.

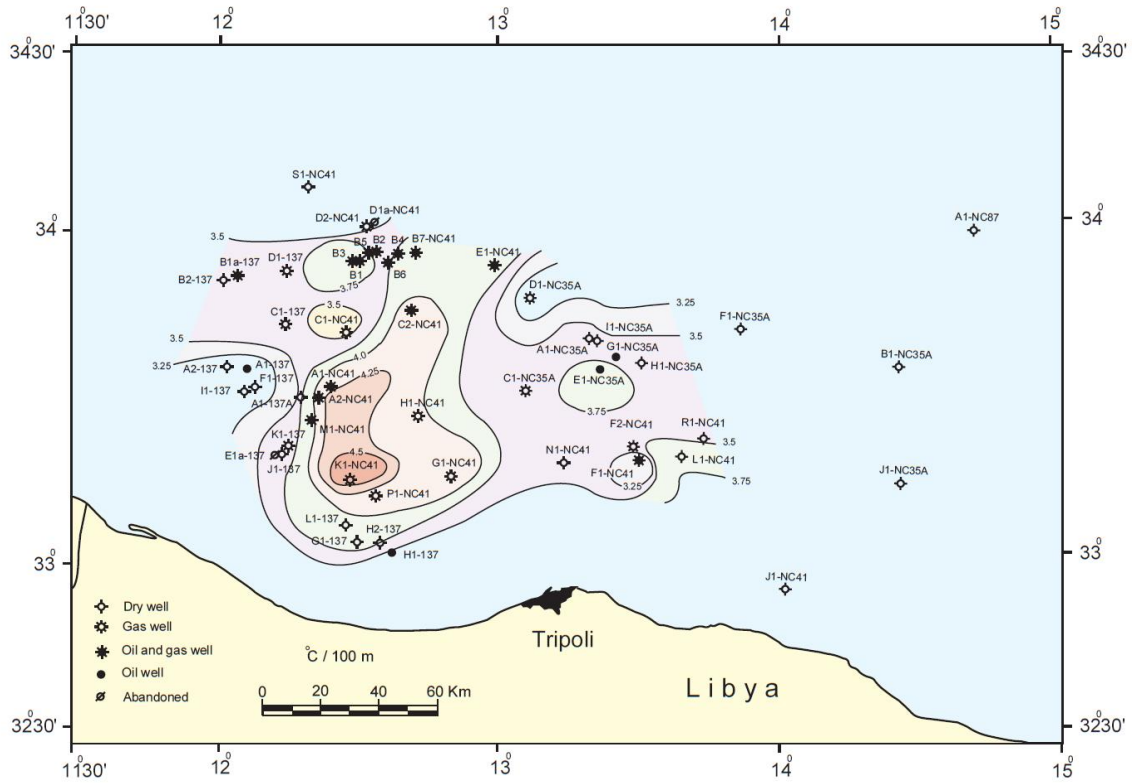


Fig. 15. Geothermal gradient map of the study area.

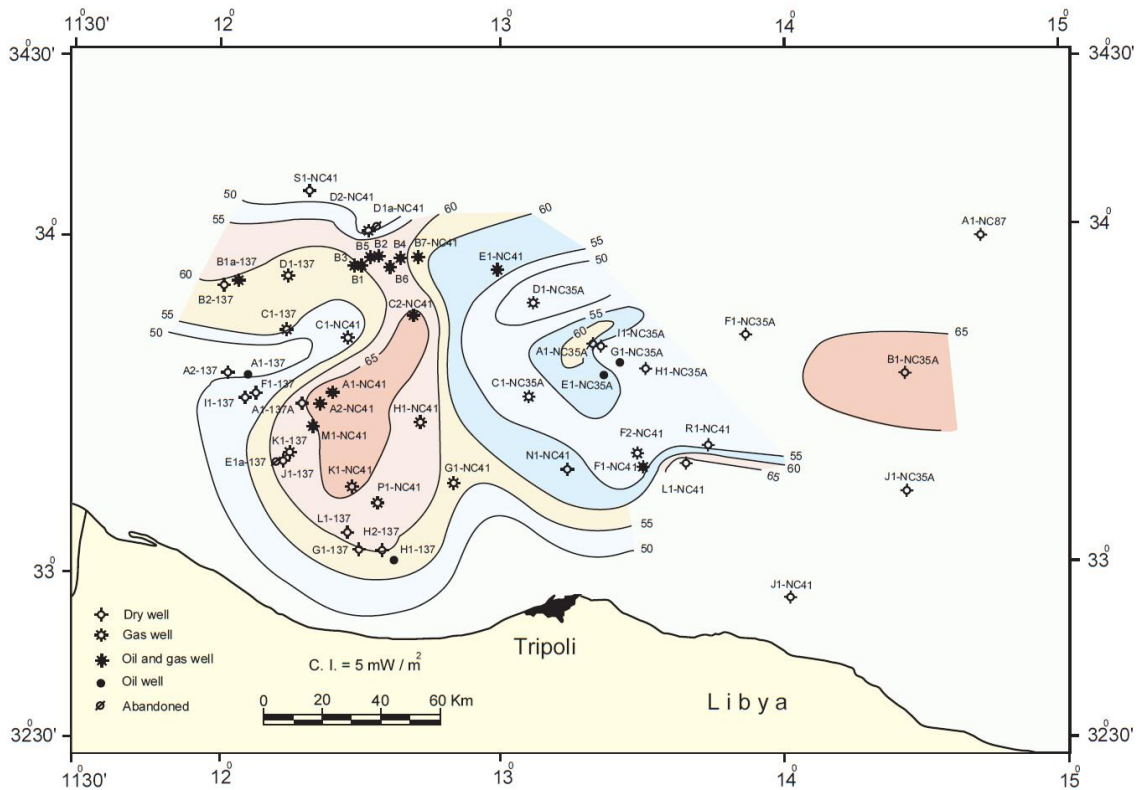


Fig. 16. Heat Flow map of the study area

5.1 Quantitative modelling of maturity data

Hydrocarbon maturation and diagenesis are functions of the thermal history of the host sediments and sedimentary rocks (McKenna and Sharp, 1998). Numerical modelling is one of the primary tools used to reconstruct this thermal history. Measured organic geochemical indices are routinely applied in the petroleum industry to determine the level of maturity of source rocks and hence to evaluate the petroleum potential of a basin. These indices reflect the cumulative effect of time and temperature on organic matter maturation and consequently can fix only the present position of the oil-generative window (OGW) (Ejedawe et al., 1984).

They are inadequate in interpreting the maturation history of a source rock or the basin (Ejedawe et al., 1984). Knowledge of the latter is important to the accurate assessment of the timing of oil generation and expulsion, and in predicting variations in the type of hydrocarbons reaching the trap at various times. To evaluate the thermal and maturation history of the G-T basin, burial history curves were constructed for 44 wells. These, (Figs. 17-20) are representative of the different thermal scenarios across the basin. Given the fact that all exploration wells from this large basin were examined in detail, the results may be considered reliable.

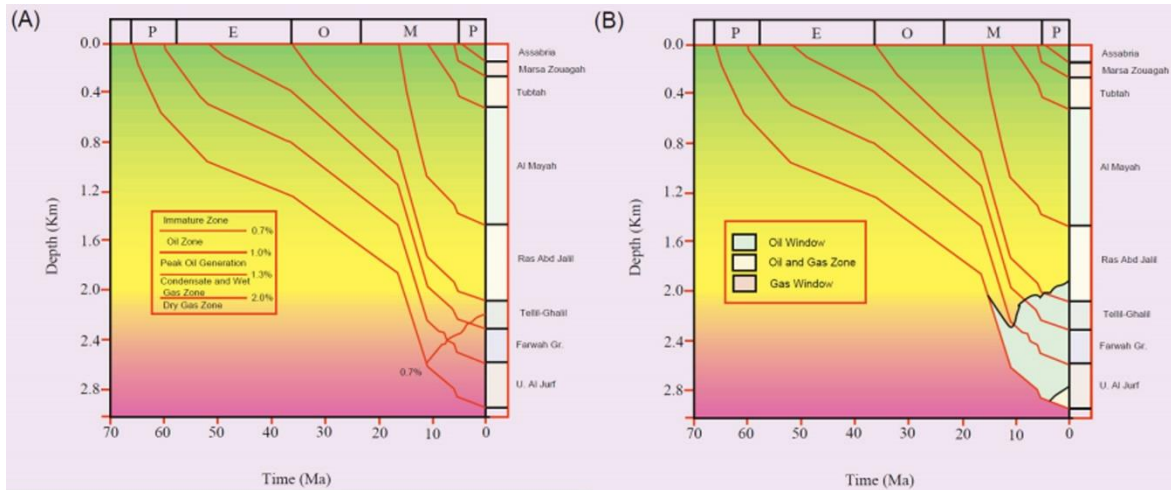


Fig. 17. Burial history curves for well B2-NC41 showing (A) Maturity windows and (B) Hydrocarbon windows

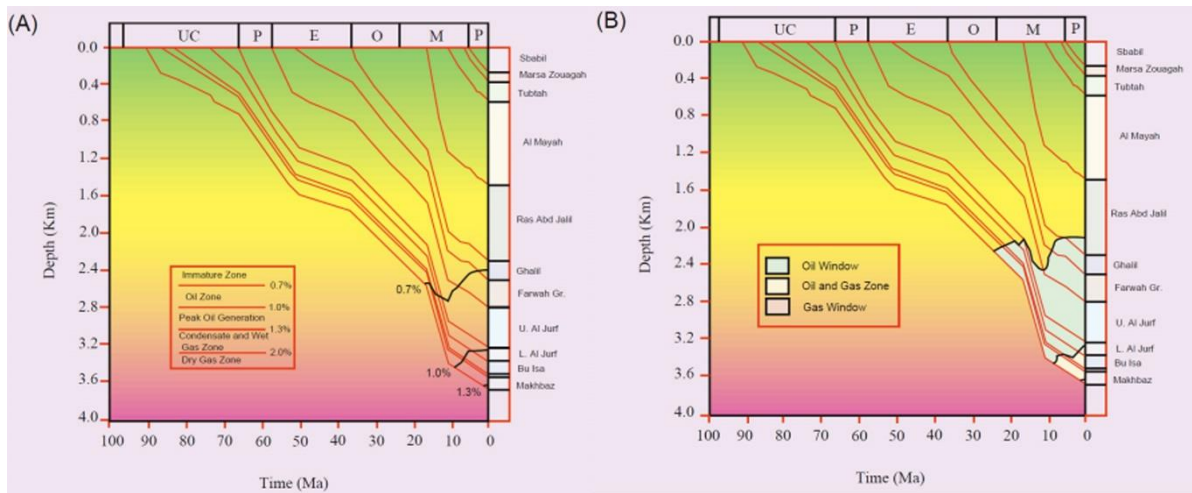


Fig. 18. Burial history curves for well D2-NC41 showing (A) Maturity windows and (B) Hydrocarbon windows

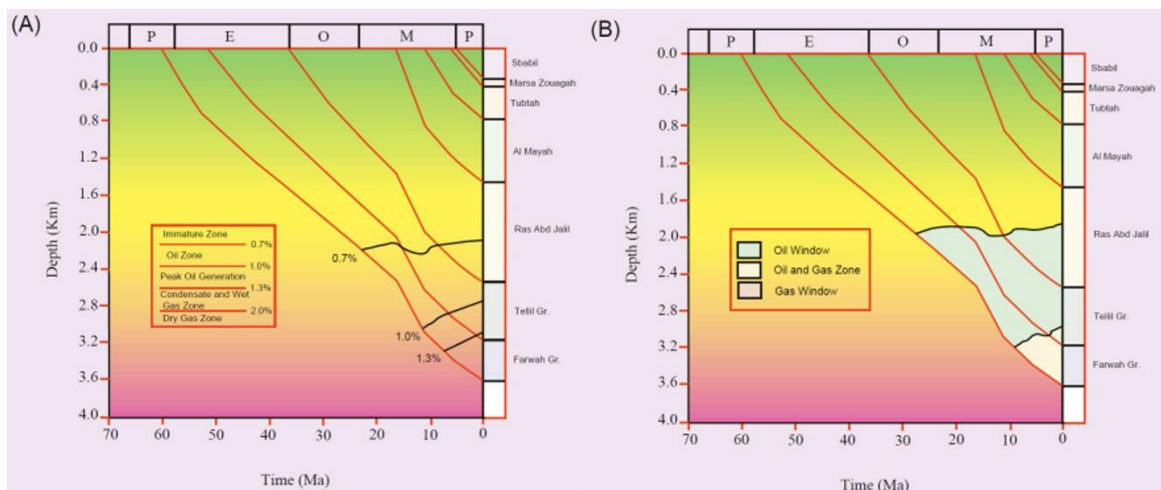


Fig. 19. Burial history curves for well H1-NC41 showing (A) Maturity windows and (B) Hydrocarbon windows

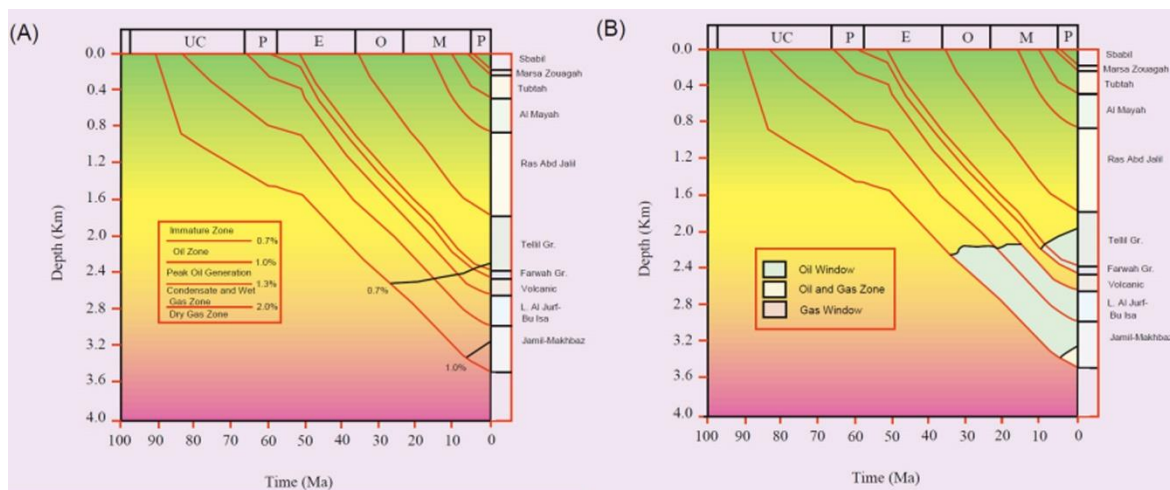


Fig. 20. Burial history curves for well H1-137 showing (A) Maturity windows and (B) Hydrocarbon windows

Thermal histories of the drilled wells were first evaluated using the corrected measured temperatures to generate a range of thermal histories compatible with the observed TAI data (Fig. 21). Calibrating heat flow and thermal conductivity to match observed subsurface temperatures is frequently done in thermal modelling. When there are no other thermal indicator data (e.g. vitrinite reflectance, T_{max} , TAI) to calibrate the thermal model, the fit to present-day temperatures is the only measure of the accuracy of the model (McKenna and Sharp, 1998). Maturation reliability is confirmed by the predicted vitrinite values, and are in accord with the observed data. The calculated Ro is in general agreement with observed thermal TAI, T_{max} and Ro. The decrease in depth to the oil window from the margin to the basin centre generally agrees with the measured geothermal gradient and heat flow.

Modelling of the B2-NC41 and D2-NC41 locations (Figs. 17-18) in the vicinity of the giant Bouri oil field and D structure respectively, indicates that the principal source rocks Farwah Group and Al Jurf formation, as well as the whole late Cretaceous sequence, are in the mature stage. The depth to the oil window at B2-NC41 and D2-NC41 wells is at 2200 and 2400 respectively. In fact, only the lower parts of the Middle-late Eocene Tellil Group has reached the Ro of 0.7% (the upper limit of the oil window). In contrast, in the central parts of the basin at H1-NC41 (Figs 19a and 19b), the model shows about 320m decrease to the top of the oil window compared with the northern margin at well D2-NC41 (Figs 18a and 18b). The depth to the main stage of oil maturity at this location is 2080 m (Fig. 19a). This depth corresponds to the middle section of the Oligocene-early Miocene Ras Abd Jalil Formation. Thus, as a result of increasing palaeoheat flow toward structurally low areas at the depocentre of the G-T Basin, sequences younger than the Eocene have entered the oil window since 8 Ma. The current depth to the top and base of the oil window ranges from 2080-3100 m giving a total thickness of 1020 m (Fig. 19a).

In contrast, at D2-NC41 location, the depth interval of the oil windows extends from 2400-3650 m giving a 1250 m thick oil zone (Fig. 18a). The model thus shows an increase of 230m in the oil window toward the northern margin from the depocentre of the basin at H1-NC41. This clearly demonstrates the impact of the thermal regime on the maturity level, thickness of oil windows, and timing of hydrocarbon generation. Modelling of the H1-NC41 well indicates that the Farwah Group was mature enough to begin generating oil in the early Miocene at 22.5 My (Fig. 19a). However, at the northern margin (B2 and D2-NC41 wells) oil was generated from the Farwah source much later at about 8 my (Figs. 17a and 18a). This is considered by this author as a crucially important result that could have a significant effect on exploration strategy in the basin.

Earlier oil generation and thinner oil zone toward the depocentre of the basin is simply explained by the constructed heat flow and geothermal pattern, which are both higher in the central parts than the basin margins (see Figs. 15 and 16). This hypothesis suggests that hydrocarbon generation at the central parts started 14 My earlier than at the basin margins. Hence, an enormous amount of this earlier-generated hydrocarbon has been subjected to secondary cracking into gas and condensate. This conclusion is supported by the explored gases and condensate fields at the central parts of the basin at H, F and C structures and liquid hydrocarbon discoveries at the Bouri structure toward the northern margin.

In the vicinity of the H1-137 location, the Farwah Group first entered the early oil maturation stage in the early Pliocene (at 5.0 Ma.), and has continued to the present (Fig. 20a). Today, the early Eocene-late Cretaceous section lies within the oil maturity window (Fig. 20b), and most of this section has been in a generative state since the end of the Oligocene (26 Ma.) (Fig. 20a). The depth interval of the zone of oil maturity (%Ro=0.7-1.0) is approximately 2300-3150 m and the base of the oil window of %Ro = 1.3 could extend to more than 3500 m (Fig. 20a). The increased depth to the top of the oil maturity zone and greater range of the zone in the northern and southern margins compared to the central basin are due to the lower heat flow over the basin margins. The earlier maturation time in the central basin is primarily a function of the higher heat flow compared to the northern and southern parts of the basin.

Modelled thermal histories that satisfy the observed maturity data (Fig. 21) indicate a gradual increase of thermal maturity with depth and lack of significant cooling episodes. Analysis of TAI, T_{max} and thermal maturation data provides some constraint on the depositional and evolutionary history of the sedimentary succession within the G-T Basin. Both measured (TAI and T_{max}) and predicted Ro maturation data for the basin indicate that palaeotemperatures were invariant and persisted without predictable changes since at least the post-rift stage. The maturity data indicate that cooling has not occurred since the deposition of the principal source rocks (late Cretaceous-early Eocene). Because significant regional uplifting and erosion during the post-rift stage is not evident, and water flow in the basin is limited, cooling has not occurred and probably the present thermal regime reflects the post-rift palaeoheat flow of the basin. However, exceptions locally exist toward the southern flanks of the basin where the stratigraphic record confirms the presence of a major gap in the sedimentary sequence from the Campanian to the Middle Eocene time during which cooling episodes possibly occurred.

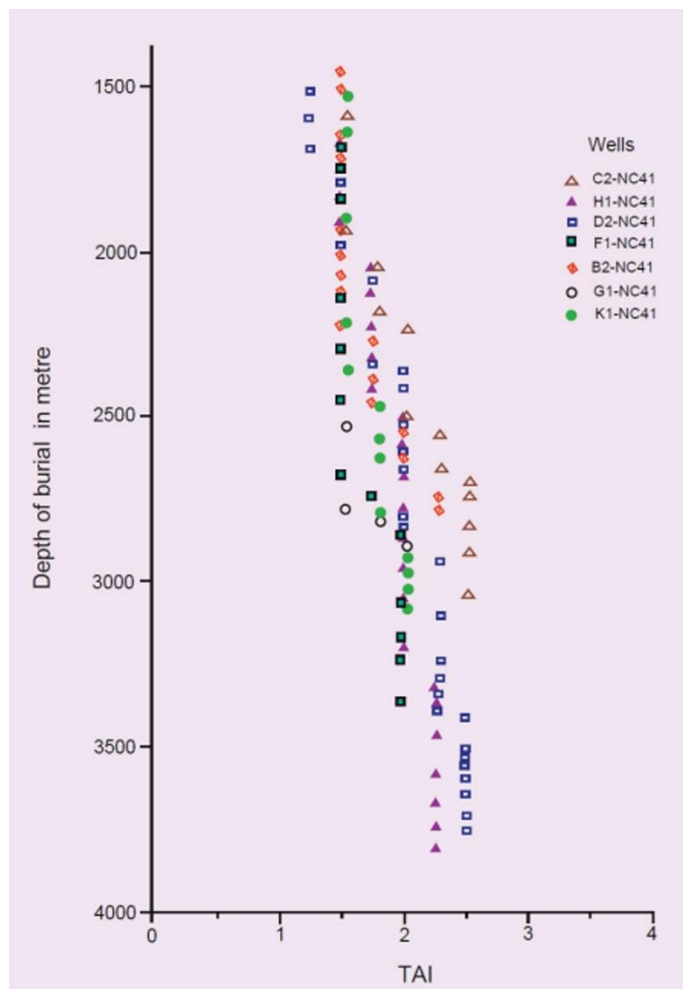


Fig. 21. Plots of the observed thermal maturity indicators (TAI) showing gradual increase of maturity with depth.

5.2 Timing of hydrocarbon generation

Geochemical analysis and basin modelling have confirmed the source rock potentiality of the early Eocene-late Cretaceous to generate hydrocarbon in the study area. They suggest that rich source intervals in both the Farwah Group and Al Jurf Formation would yield major oil and gas to associated reservoirs. Based on the interpreted thermal regime and thermal maturation levels the main Petroleum kitchen has been mapped within the G-T Basin. The area of major hydrocarbon generation occupies the central parts of the basin (Fig. 22 and 23). It has the capacity to generate major hydrocarbons, which have undergone a short-range migration to fill the Eocene Farwah and Tellil reservoirs. It is proposed here that hydrocarbon has been generated in a wide span of time and from several proven organic-rich sources, which have been encountered at various drilling depths. The impact of the thermal regime and temperature structure proposed in this study is conspicuously manifested in variation across the basin of the timing of hydrocarbon generation, of depth to the oil window and depth interval of the oil zones. The results match observed petroleum occurrences in the G-T Basin and can be used as a sensible approach to assess migration pattern and reduce exploration risk in the study area. Hydrocarbon has been generated from the Al Jurf and Farwah sources during Oligocene and early Miocene in the central G-T Basin. The model shows that hydrocarbon in the H1-NC41 location has been initiated at 22.5 my from Farwah source and probably at about 30 my from the Al Jurf source (Fig. 19a). Both of the principal source rocks are presently at the condensate and wet gas zone ($R_o = 1.3-2.0\%$). However, at the northern margin of the basin, toward the vicinity of D2-NC41 location (Fig. 18a), the Al Jurf Formation has reached the peak of oil generation ($R_o=1.0-1.3\%$) and the timing of oil generation from this source began 14 my ago (later than the central basin by 16 my). This

scenario is repeated toward the southern margin at well H1-137 (Fig. 20a) where the Al Jurf Formation started to generate hydrocarbon since only 15 my ago, again much later (by 15 my) than generation time at the basin depocentre. The model also indicates that the late Cretaceous-Palaeocene Al Jurf Formation is in the early stage of thermal maturity in the oil zone i.e. $R_o = 0.7-1.0\%$. This result matches with the observed oil shows that have been found at H1-137 well. Similar results, however, are obtained when the second important source, the Farwah Group, is examined. Hydrocarbon generation from the group source at the northern margin (D2-NC41) (Fig. 18a) and the southern margin (H1-137) (Fig. 20a) of the G-T Basin, commenced at 8 my and 5 my respectively and in both locations the group is in the early stage of thermal maturation ($R_o=0.7-1.0\%$). Nevertheless, at the central parts of the basin (H1-NC41), hydrocarbon generation started at 22.5 my ago (Fig. 19a). A time difference ranging between 14.5-17.5 my occurs from the basin centre to the margins. Thus, basin modelling yields consistent results and clearly matches with the observed petroleum occurrence, which is, gas discoveries at the central parts and liquid hydrocarbon accumulations toward the north and minor, but also liquid, accumulations at the southern parts. These facts have crucially important strategic values in the near future petroleum exploration programs. Most known traps were formed post-Eocene, and the major generation-migration and accumulation of petroleum commenced during early Miocene and continues to the present; however, the timing of oil generation for each of the potential source rocks varies throughout the study area as a function of the heat flow and depth of burial. Because of the timing of peak oil generation varies spatially, overlaps in the timing of generation exist among the different source rocks. This relationship enhances the prospectivity of this area because it allows late migration in multiple source rocks, and early migration and accumulation into numerous porous Eocene reservoirs. The structural traps within or close to the interpreted petroleum kitchen are here rated as highly prospective. Exploration risks generally increase with the distance from the principal area of hydrocarbon generation and significant hydrocarbon accumulation are remained to be discovered in the basin.

In conclusion, basin modelling results and burial history analysis of the G-T Basin show that hydrocarbon generation took place during a wide time span. It has been found that oil started to generate in the basin depocentre from the principal Al Jurf and Farwah sources during 30 and 22.5 my respectively but at the northern and southern margins it started some 15 my later. Since then hydrocarbon has migrated out of the basin depocentre, where the main petroleum kitchen is located, toward the basin flanks in a radial pathway pattern. However, an enormous amount of oil has also been proven to be generated and expelled out of the Al Jurf and Farwah Groups within the northern flanks. Thus, most but not the entire liquid hydrocarbon in the vicinity of the giant Bouri oil field probably originated from these.

Variation of palaeoheat flow undoubtedly controlled the changes in the timing of hydrocarbon generation across the basin and depth to the top of the oil windows as well as the depth interval of the different hydrocarbon liquid and gas windows. The present-day heat-flow regime is a key factor to the understanding of the hydrocarbon habitat in the basin and offers a valid answer to the explorationist as to where, how and when hydrocarbon can be found in the basin. The difference between the timing of oil generation and the beginning of Farwah source rocks deposition is more than 40 my, which indicates that a normal rather than high palaeoheat flow regime prevailed since source rocks deposition. It is found that in basins of high heat flow i.e. Pattani Basin, Gulf of Thailand, hydrocarbon generation started since 5-7 m.y. after deposition (Bustin and Chonchawalit, 1997).

5.3 Source rock potential of the G-T Basin

Source rock maturity maps are presented for the Middle-Upper Eocene, late Palaeocene-early Eocene and Maastrichtian-Palaeo-

cene sequences in terms of vitrinite values (Figs. 22-24). The maturity maps were constructed using all available geochemical data, the basis of which is derived from Agip oil company and Petroleum Research Centre labs (Rock-Eval pyrolysis data on well A1-NC35A). All types of maturity indicators were considered including thermal

alteration index (TAI), actual vitrinite reflectance and Rock-Eval pyrolysis Tmax. Two principal rock intervals are recognized in the study area. They are the Al Jurf formation and the Bilal formation of the Farwah Group. Both intervals are classified as very good source rocks.

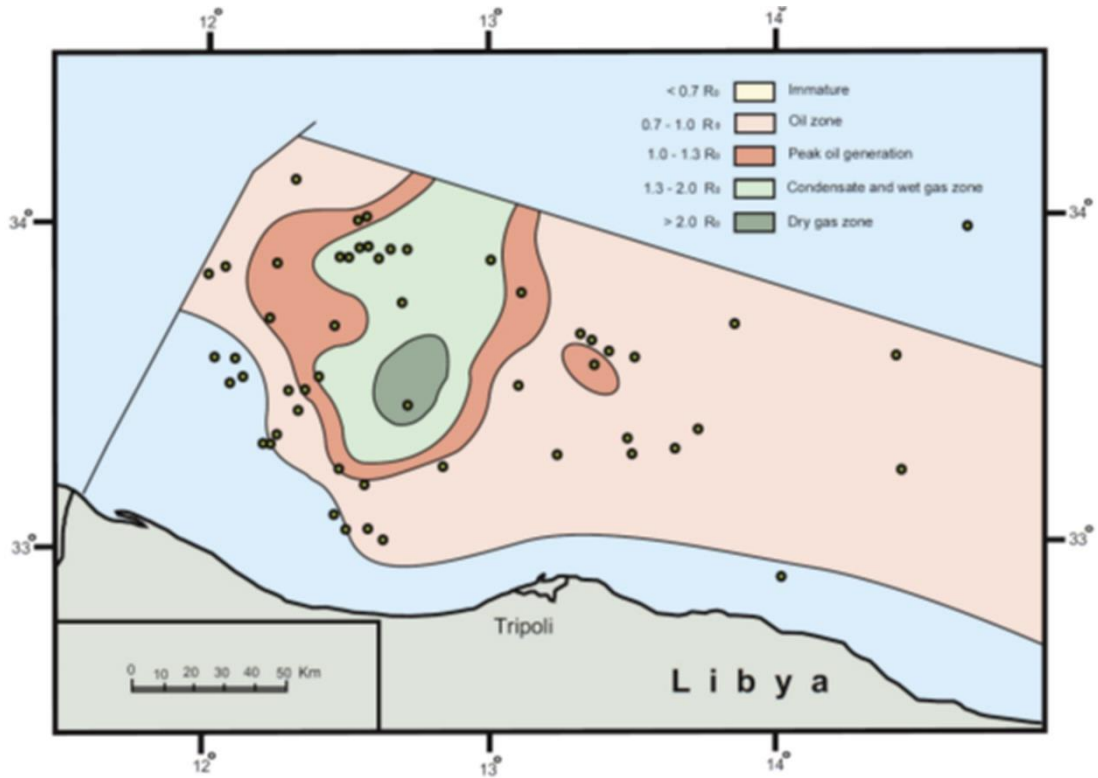


Fig. 22. Thermal maturity of the base of the lower Aljurf formation at 0.0 Ma

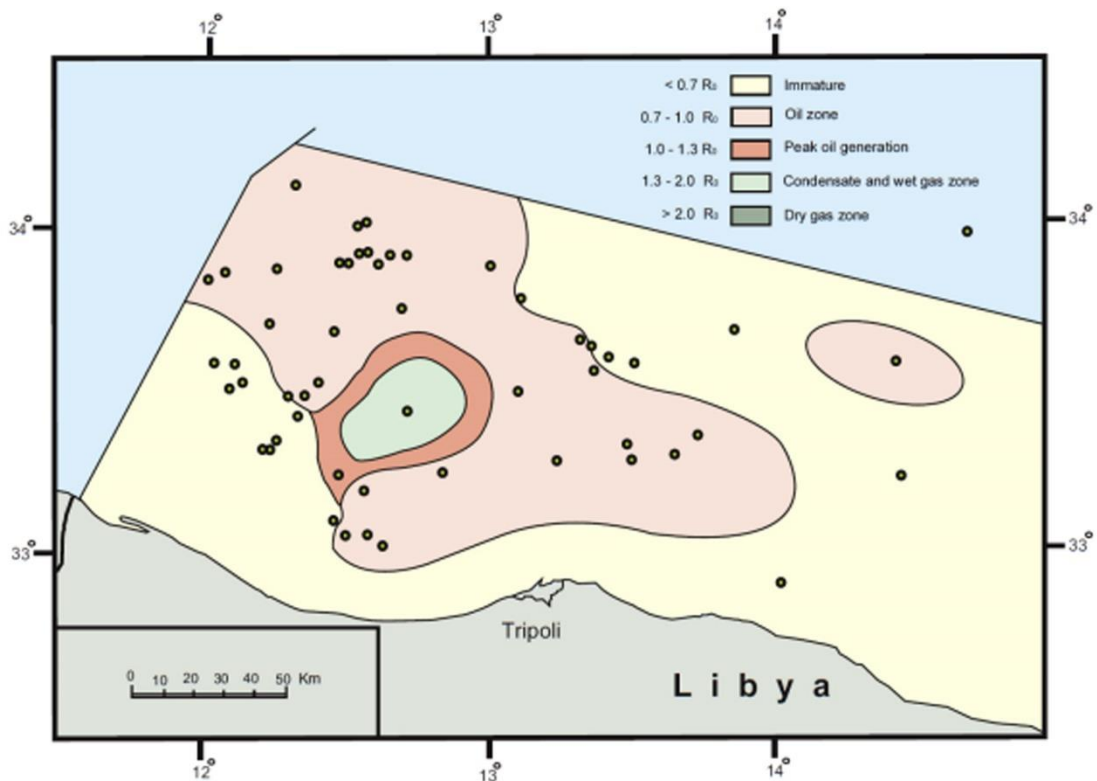


Fig. 23. Thermal maturity of the base of the Farwah group at 0.0 Ma

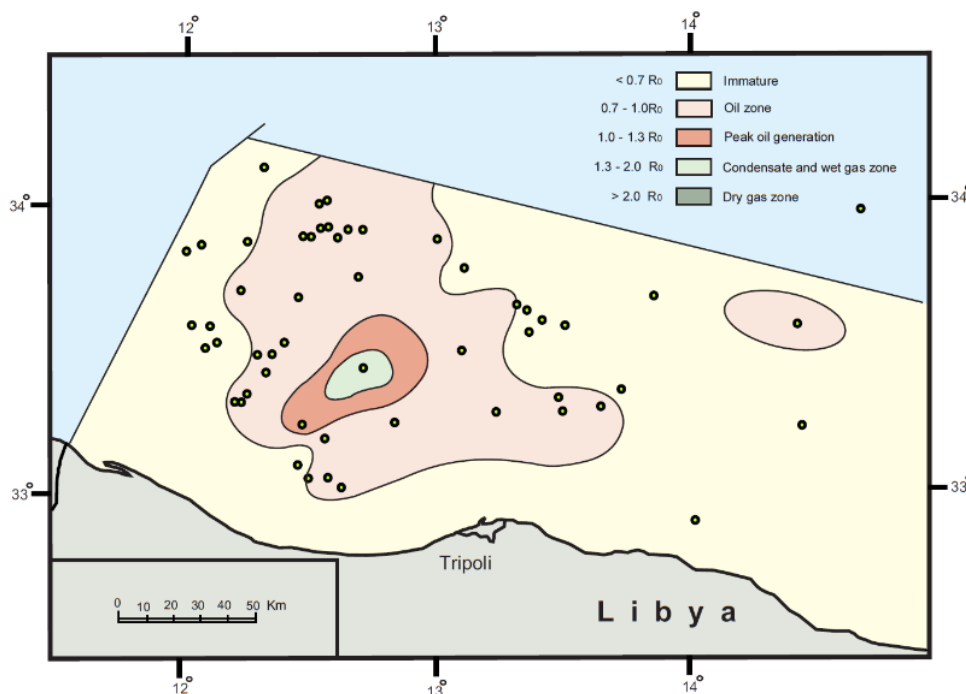


Fig. 24. Thermal maturity of the base of the Tellil group at 0.0 Ma

For mapping purposes, all maturity data are presented in vitrinite reflectance values. The constructed maturity maps of the late Cretaceous-Palaeogene sequences were prepared to show maturity levels referred to the present time. Data concerning the sequences were available from all exploration wells at 44 locations distributed over all the basin, therefore the maps constructed can be considered reliable. Maturity windows are almost similar to that of Tissot and Welte (1984) and were defined as follows:

- < 0.7 Ro immature
- 0.7-1.0 Ro oil zone
- 1.0-1.3 Ro peak oil generation
- 1.3-2.0 Ro condensate and wet gas
- > 2.0 Ro dry gas zone

5.3.1 Source potential of the Al Jurf Formation

The Maastrichtian lower Al Jurf formation is comprised of deep shales and limestones with planktonic foraminifera. The quality of the kerogen evaluated geochemically from 13 wells in the basin shows that the upper and lower Al Jurf formations are composed of fair to very good quality source rocks with levels of excellent potential to generate hydrocarbon i.e. at wells B1 and C1-NC41. The maturity maps related to the base of the Lower Al Jurf Formation show the complete maturation of the area (Fig. 22). The constructed maturity maps show a central over mature zone in the deep parts of the basin ($Ro = 1.3-2.0$ and > 2.0) surrounded by a narrow belt of mature facies in the peak of oil generation ($Ro = 1.0-1.3$). These zones then pass laterally into mature facies in the oil zone ($Ro = 0.7-1.0$) over all parts of the basin.

5.3.2 Source potential of the Farwah Group

The late Palaeocene-early Eocene Bilal Formation of the Farwah Group contains a good petroleum source potential. TOC contents from geochemical analysis of 13 wells reveal fair-very good organic richness in the range of 0.2-4.74%. This formation is mature-overmature in most parts of the basin and is actively generating oil at present. Kerogen content is highly oil and gas prone and basically comprises continental herbaceous phytoclasts, continental woody debris and amorphous organic matter. The maturity map for the late Palaeocene-early Eocene, of the Bilal Formation (Fig. 23) shows large portions of the G-T Basin are immature ($Ro = < 0.7$). The immature areas are well established toward the east, south and almost the northeastern parts of the basin. Nevertheless, mature zone

($Ro = 0.7-1.0$) extends over large areas of the central basin (Fig. 23) and coincides generally with areas of relatively higher heat flow. Locally, toward the centre at H1-NC41 location, the sequence attained over mature stage and is in the condensate and wet gas zone ($Ro = 1.3-2.0$). Lower maturity values in the southern, eastern and northern G-T Basin can be attributed to the higher structural position and lower heat flow through time relative to the deeper central G-T Basin.

5.3.3 Source potential of the Tellil Group

The Middle-Upper Eocene Tellil Group is generally of poor-fair quality source rock. In most parts of the study area, the TOC ranges from 0.2-0.8%. The sequence is either immature or mature locally in its lower part. Since it is lean in organic carbon, and in many parts of the basin, only partially mature, it is not considered as important as the earlier deposited sequences of Farwah and Al Jurf. The maturity map (Fig. 24) of the Tellil Group clearly mimics the same pattern of the Farwah Group (Fig. 23), and is again consistent with the modelled thermal regime and temperature structure of the basin. The maturity map (Fig. 24) shows a large mature area in the oil zone ($Ro = 0.7-1.0$) located in the basin depocentre and coincides with the interpreted principal petroleum kitchen of the basin which delineates the area of highest heat flow. A narrow belt exhibiting a bull's eye closure of mature and over mature zones is present at the basin centre (Fig. 24). Although, the group is in the mature stage over large areas in the central parts, its hydrocarbon potentiality is not considered here. This is because the shallow shelf carbonates and shales have poor source potential with an average of less than 0.5% and basin modelling yields strong evidence that the sequence is not capable of expelling hydrocarbon. The hydrogen index measured at well A1-NC35A is less than 100 and the type of organic matter in most parts of the basin comprises of rare algae and a mixture of continental herbaceous and woody debris with amorphous materials that indicate the environment of deposition was anoxic.

5.3.4 Hydrocarbon potential of other source rocks

In most parts of the study area, all the Eocene and late Cretaceous source rocks are mature or overmature but only the Farwah and Al Jurf formation are organically rich enough to generate and expel major quantities of hydrocarbon. However, the possibility of other older sources is not ruled out. This is supported by the fact that in many parts of the basin they have not been penetrated by

drilling. Moreover, in a few cases, however, when they have been encountered and geochemically analyzed. Geochemical evidence from the Tunisian extension of the G-T Basin, have confirmed the source rock potentiality of Cenomanian-Turonian limestones of the Bahloul formation (Ben Ferjani *et al.*, 1990). It is considered as the main source rock for the late Cretaceous reservoirs and for the early Eocene reservoir where tectonics allow the migration of the Bahloul oil into the Ypresian reservoir.

It is crucially important to mention that, the early Eocene Bou Dabbous Formation (equivalent to Hallab Formation in Libyan offshore) source for the offshore oils implies either the absence of Cretaceous-based petroleum system or the presence of an effective seal, which prevents Cretaceous-derived oils from reaching Tertiary reservoirs in the Gulf of Gabes. The occurrence of Cretaceous-derived oils immediately onshore suggests the latter possibility is the case and makes pre-Tertiary reservoirs attractive targets in the offshore (Hughes and Reed, 1995). If this hypothesis is true then the difference between the early Tertiary and late Cretaceous pressure systems in the Libyan offshore may simply be attributed to the presence of the same seal between the two systems. It is here proposed that the potentiality of the late Cretaceous reservoirs is similarly augmented in the Libyan offshore and that enormous amount of hydrocarbon yet remain to be discovered within the basin. For the first time, a new temperature structure and thermal regime have been constructed based on corrected BHT and are consistent with observed thermal maturity indicators. This new heat flow regime is remarkably lower than that of the AGIP oil company (Benelli, *et al.*, 1985) as the long time lapse between source rock deposition and hydrocarbon generation would suggest. This fact enhances the chance of finding more liquid hydrocarbon within the basin.

6. Summary and conclusions

The G-T Basin is a Mesozoic-Cenozoic basin which was initiated as a result of widespread, late Triassic, Jurassic and early Cretaceous extensional movements that developed over a broad zone of strain between the African and European plates. A detailed facies and sequence analysis carried out in the G-T Basin has resulted in a stratigraphic correlation scheme and construction of depositional models for the entire Mesozoic-Cenozoic succession. The sedimentary sequences forming the bulk stratigraphy of the G-T Basin comprises a 10 km-thick succession of Early-Middle Triassic, nonmarine and marine clastics, late Triassic-Middle Jurassic, predominantly shallow marine carbonates and evaporites and Middle Jurassic-Recent marine carbonates and clastics. The tectono-stratigraphic units comprise 7 sequences on the time scale of second-order sequences. For most sequences and sequence boundaries, either a eustatic or tectonically enhanced origin can be established.

The analysis of the basin-fill history of the G-T Basin from the Triassic until the Holocene reveals that the basin underwent development from a continental sedimentary basin located on Gondwana to an epicratonic rift basin. When major extensional movements ceased (late Cretaceous), the basin subsided thermally and developed as part of a passive continental margin on the North African plate margin. The basin also has been subjected to strike slip movements and compressional events lead to inversion during the late Cretaceous and Eocene time. The dominant driving mechanism of subsidence clearly seems to have been subsidence due to cooling following lithospheric thinning and the tectonic subsidence history shows that a simple stretching model successfully predicts the overall characteristics of the long-term patterns of the tectonic subsidence of the basin. Regional deep seismic reflection profiles in the G-T Basin shows that the Moho shallows from 32 km beneath the unrifted coastal

region to about 26 km below other parts of the basin. The observed stretching factor, in the range $\beta=1.38-2.33$, corresponds to a crustal extension of 38-133%. The highest values of the stretching factor are associated with the basin centre; values diminish outward toward the basin margins. The region of greatest thinning is directly below the region of greatest sedimentary thickness in the G-T Basin depocentre.

The crust has been thinned a half and less than a half of its original thickness at the central and northern parts respectively and only thinned to a quarter of its original thickness at the coastal region. The central and northern regions of the basin have similar stretching values; however, the central area is characterized by the older timing of HC generation and shallower depth of the oil window. In another words, similar stretching factor but different depth of maturity windows and different timing of HC generation characterize these areas. Therefore, crustal nature (age and composition) cause important HF variations and depth of burial is causing spatial variation in the depth of HC window within the G-T Basin. Hence, both the proposed stretching hypothesis as well as depth of burial are useful exploration tool in the basin and are considered as paramount to the understanding of basin evolution and hydrocarbon accumulation.

The observed organic thermal maturity measurements in the G-T Basin indicate that the pre-Middle Eocene sequences are at a mature to over mature stage. The Middle-Upper Eocene Tellil sequence attained an early mature stage while locally the Oligocene-Early Miocene is in a mature stage. The rest of the Tertiary sequence is immature. The depth variation to the modelled top of the oil maturity 0.7 Ro ranges from 2000-2400 m in the G-T Basin. The highest Ro maturity values in the principal source rocks (Farwah and Al Jurf) are in the basin centre, and that Ro values change gradually toward the basin margins. This anomaly is attributed to the spatial variation in depth of burial and crustal thinning toward the basin centre, as is witnessed by the deep seismic interpretation across the basin.

The calculated organic maturities indicate that the early Eocene-late Cretaceous sequences are either mature or over mature with respect to the oil window. The current depth to the top of the oil window ranges from 2000 to 2400m, and the base of the oil window ranges from 3000 to 3650 m. Combined geohistory and basin modelling indicates that the main phase of hydrocarbon generation from the Farwah source began 22.5 to 5.0 Ma, and continues until the present. A relatively late generation (approximately 30-50 my after deposition) is ascribed to the lack of high palaeoheat flow and moderate burial, which is consistent with a passive margin and post-rift thermally subsiding basin. Hydrocarbon has been generated from the Al Jurf and Farwah sources in the basin centre first and earlier than the basin margins by about 15 my. Hydrocarbon generation commenced about 30 my from the Al Jurf Formation and at 22.5 my from the Farwah source in the basin centre. It began, however, to generate 15 my later from both principal sources at the basin margins.

6. Acknowledgments

Editors of the 2nd International Conference on Geosciences of Libya reviewed the manuscript and made helpful suggestions and comments. The author wish to thank the management of the National Oil Corporation (NOC) for the sponsorship and permission to publish the data and interpretations in

this paper. A major part of this work was carried out at the Earth Sciences department of the University of Manchester as part of the requirements for a PhD under the supervision of Dr. Mike Anketell. His support and encouragement are greatly appreciated. Further improvements of the results were added to the discussion based on the author working experience in the Mediterranean region.

References

- Allen, P. A. and Allen, J. R. (1990) Basin analysis principles and applications. Blackwell Scientific Publications, London, 451p.
- Benelli, F., Mcavaggion, M. and El Ashuri, O. (1985) Oil habitat in concession NC41, Agip N.A.M.E., Tripoli.
- Bustin, R. M. and Chonchawalit, A. (1997) 'Petroleum source rock potential and evolution of Tertiary strata, Pattani Basin, Gulf of Thailand', *Am. Assoc. Petrol. Geologists*, 81, pp. 2000-2023.
- Ejedawe, J. E., Coker, S. J. L., Lambert-Aikhionbare, D. O., Alfofe, K. B. and Adoh, F. O. (1984) 'Evolution of oil-generative window and oil and gas occurrence in Tertiary Niger Delta basin', *Am. Assoc. Petrol. Geologists*, 68, pp. 1744-1751.
- Falvey, D. A. and Mutter, J. C. (1981) 'Regional plate tectonics and the evolution of Australia's passive continental margins', *BMR Journal of Australian Geology and Geophysics*, 6, pp. 1-29.
- Faux, F. A., Johnson, W. R., Kienzle, J. K. and Mcdowell, E. H. (1988) Regional Geophysical studies. In: Mccrossan, R. G. and Booth, J. E. (eds.) *Geology of western offshore Libya and adjacent regions*. Sirt Oil Company, 1, pp. 37-79.
- Hammuda, O. S., Sbeta, A. M., Mouzughi, A. J. and Eliagoubi, B. A. (1985) *Stratigraphic Nomenclature of the north-western offshore of Libya*. The Earth Sciences Society of Libya, Tarabulus, Libya, 166p.
- Haq, B. U., Hardenbol, J. and Vail, P. R. (1987) 'Chronology of fluctuating sea levels since the Triassic', *Science*, 235, pp. 1156-1167.
- Hughes, W. B. and Reed, J. D. (1995) Oil and source rock geochemistry and exploration implications in the northern Tunisia. In: *The proceedings of the seminar on source rocks and hydrocarbon habitat in Tunisia*, ETAP, Memoir No. 9, pp. 49-67.
- Institute Francais Du Petrole. (1995) Genex user's guid. An IFP basin modelling software, marketed and maintained by Beicip-Franlab.
- Lopitan, N. V. (1971) 'Temperature and geologic time as factors in coalification', *Akad. Nauk, SSSR, Izv. Ser. Geol.*, 3, pp. 95-106.
- Mckenna, T. E. and Sharp, J. M. (1998) 'Radiogenic heat production in sedimentary rocks of the Gulf of Mexico Basin, South Texas', *Am. Assoc. Petrol. Geologists*, 82, pp. 484-496.
- Mckenzie, D. (1978) 'Some remarks on the development of sedimentary basins', *Earth and Planetary Science Letters*, 40, pp. 25-32.
- Mriheel, I.Y. and El Bakai, M. T. (1992) Petroleum geology of the Western Libyan offshore (Abstract). In: *the 29th International Geological Congress*, Kyoto, Japan.
- Mriheel, I. Y. and Alhnaish, A. S. (1995) 'Study of the Mesinian carbonate-evaporite lithofacies offshore Western Libya', *Terra Nova*, 7, pp. 213-220.
- Mriheel, I. Y. (2000) 'Basin Modelling and Reservoir Geology of the Principal Reservoir, Farwah Group, Gabes-Tripoli Basin, Western Offshore, Libya', *PhD. thesis*, Manchester University, UK.
- Mriheel, I. Y. (2013) Jennawen Formation, a new stratigraphic unit at Jifarah Escarpment, Western Libya. *Report*, 5 p.
- Mriheel, I. Y. (2014) Paleogeography and Sedimentation History of the Western Libya Offshore, Central Mediterranean (Extended Abstract). In: *The International Conference and Exhibition, Am. Assoc. Petrol. Geologists*, Istanbul, Turkey
- Steckler, M. S. and Watts, A. B. (1978) 'Subsidence of the Atlantic-type continental margin of New Yourk', *Earth and Planetary Science Letters*, 41, pp. 1-13.
- Tissot, B. P. and Espitalie, J. (1975) L'évolution thermique de la matiere organique des sediments: applications d'une simulation mathematique: *Revue de l' Institut Francais du Petrole*, 30, pp. 743-777.
- Tissot, B. P. and Welte, D.W. (1984) *Petroleum formation and occurrence*, 2nd edition. Springer-Verlag, Berlin-Heidelberg-New York, 699p.
- Ungerer, P., Espitalie, J., Behar, F. and Eggen, S. (1988) Modelization mathematique des interactions entre craquage thermique et migration lors de la formation du petrole et du gaz: *Compte Rendu a l'Academie des Sciences, serie II*, p. p. 927-934.